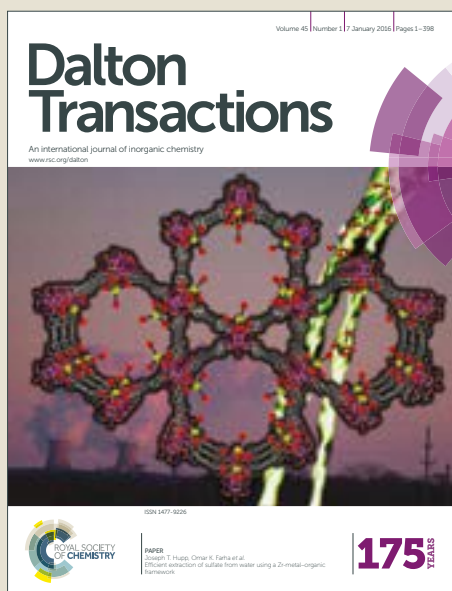


Dalton Transactions

Accepted Manuscript



This article can be cited before page numbers have been issued, to do this please use: S. J. Raynes, M. A. Shah and R. A. Taylor, *Dalton Trans.*, 2019, DOI: 10.1039/C9DT00922A.



This is an Accepted Manuscript, which has been through the Royal Society of Chemistry peer review process and has been accepted for publication.

Accepted Manuscripts are published online shortly after acceptance, before technical editing, formatting and proof reading. Using this free service, authors can make their results available to the community, in citable form, before we publish the edited article. We will replace this Accepted Manuscript with the edited and formatted Advance Article as soon as it is available.

You can find more information about Accepted Manuscripts in the [author guidelines](#).

Please note that technical editing may introduce minor changes to the text and/or graphics, which may alter content. The journal's standard [Terms & Conditions](#) and the ethical guidelines, outlined in our [author and reviewer resource centre](#), still apply. In no event shall the Royal Society of Chemistry be held responsible for any errors or omissions in this Accepted Manuscript or any consequences arising from the use of any information it contains.

Direct conversion of methane to methanol with zeolites: towards understanding the role of extra-framework d-block metal and zeolite framework type

Received 00th January 20xx,
Accepted 00th January 20xx

DOI: 10.1039/x0xx00000x

www.rsc.org/

Samuel Raynes^a, Meera Shah^a and Russell A. Taylor^{a*}

The direct conversion of methane to methanol has been an active area of research for over a century, though a viable industrial process is yet to be realised. However, in the last three decades substantial progress has been made in the field through homogeneous and heterogeneous approaches. This perspective article explores the latest advances in the field of direct methane to methanol conversion by zeolites containing extraframework d-block metals, focussing on first row, d-block metals. The article highlights the similarities and differences in the nature and formation of the active site, the mechanism of methane activation as well as mode of functionalisation, and where appropriate draws on understanding gained from theoretical studies. From the insight obtained into the different roles of the extra-framework metal and zeolite framework we propose new areas of research which the authors believe will be of benefit to the field.

1. Introduction

Methane, the principle component of natural gas, continues to play an ever increasing role as a feedstock for the production of energy and chemicals.¹ While energy production remains the primary use of methane, it is also the feedstock for some of the most important inorganic and organic bulk chemicals produced by the chemical industry. However, bulk chemicals are not produced directly from methane but are instead produced indirectly through the intermediacy of synthesis gas (also known as syngas), a mixture of carbon monoxide and hydrogen. Figure 1 shows some of the diverse bulk chemicals that are produced from synthesis gas, either by utilising hydrogen or carbon monoxide alone, or by using syngas.

Syngas can be produced from methane in a number of ways² but steam reforming (SR) and autothermal reforming

(ATR, a combination of steam reforming and partial oxidation) remain the most practised methods.^{3,4} Historically it is steam reforming that has been most commonly implemented for producing syngas for the manufacture of important basic chemicals (e.g., ammonia and methanol), oil refining, and in many other industrial applications.⁵

The industrially practised approach for converting methane to chemicals *via* syngas has a number of drawbacks. Both SR and ATR of methane utilise catalysts and operate at elevated temperature (800 °C and above) and pressures (30 barg and above).⁵ Due to these extreme conditions, plant construction costs are high and the catalysts are prone to deactivation due to sintering or the formation of carbonaceous deposits.² Furthermore, depending on the degree of heat exchange, it is estimated that approximately between 20% and 50% of the natural gas feedstock is consumed through energy losses in order to reach the high reaction temperatures required during SR.³ Further it is reported that trying to improve the energy efficiency of SR would detrimentally impact the syngas production cost.⁶ Given the points above, syngas production plants are typically constructed at large scales to optimise material throughput and thus maximise the return on investment. As it stands today, the conversion of methane to

^a Department of Chemistry, Durham University, South Road, Durham DH1 3LE, United Kingdom

Electronic Supplementary Information (ESI) available: [details of any supplementary information available should be included here]. See DOI: 10.1039/x0xx00000x



Samuel Raynes

Samuel Raynes received his Masters degree in chemistry from Durham University in 2017. He is now pursuing a Ph.D. with Dr. Russell Taylor where his research centres on the use of multifunctional zeolite materials for the cascade conversion of bio-derived small molecules.



Meera Shah

Meera Shah received her Masters degree in Natural Sciences from Durham University in 2016. She is currently pursuing a Ph.D. with Dr. Russell Taylor focusing on methane activation and functionalisation over zinc-modified zeolite materials.

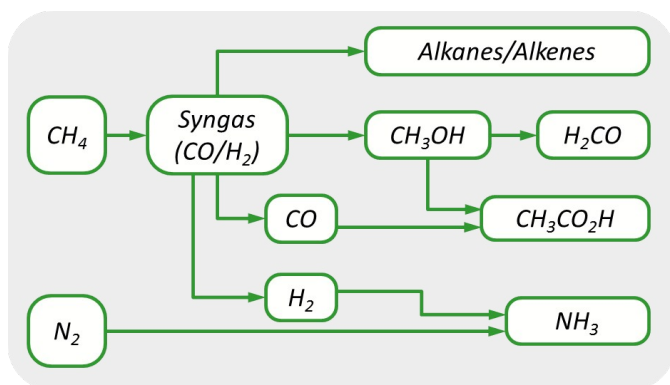


Figure 1: Flow scheme showing some of the primary products formed from syngas.

chemical products requires a minimum of two chemical manufacturing plants, of which syngas production reportedly accounts for the majority of the investment required. For instance, the production of methanol from methane requires a syngas production plant and a methanol synthesis plant where the latter most commonly utilises a Cu/ZnO/Al₂O₃ catalyst to produce the desired product.⁷ For methanol production, the syngas plant accounts for approximately 60% of a new production facility.³ This multistep, large scale approach consequently limits the number of opportunities for deployment of indirect methane conversion technology.

The direct conversion of methane to higher value chemical products has been an area of industrial and academic interest ever since the turn of the 20th century.⁸ Moreover the prospect of direct conversion to liquid products has the allure of being able to address two important areas that indirect production cannot. Firstly, associated natural gas (gas produced at oil reservoirs) is often flared on site for environmental and safety reasons, however, in 2015, this amounted to approximately 3.5% of global gas production.⁹ Secondly, it is estimated that 40% of natural gas reserves are not economically viable resources as the cost of production is too significant compared to the perceived financial reward.¹⁰ Such reserves are known as stranded gas. The direct conversion of methane to higher value chemicals has the



Russell A. Taylor

Fellowship to develop novel hydrocarbon conversion processes. Research in his group focuses on the development of new catalytic materials and catalytic processes for small molecule conversion.

Russell Taylor obtained his PhD in 2007 from Imperial College London (UK) having studied platinum mediated, homogeneous methane oxidation. He subsequently joined BP in 2008, working at the R&D centre in Hull (UK). His research at BP spanned homogeneous catalysis as well as zeolite mediated catalysis and process development. In September 2015 Russell became an Assistant Professor at Durham University (UK), and in 2018 he was awarded an EPSRC Manufacturing

potential to tap into these resources should the requisite plants have lower associated costs than indirect production (such as capital expenditure (CAPEX) and/or operating expenditure (OPEX)). There are of course serious concerns regarding the exploitation of coal, oil and gas for fuels and chemicals, mainly due to the risks of global warming and other environmental issues.¹¹⁻¹³ However, natural gas is regarded as the cleanest of all the fossil based resources and is championed to be the preferred resource in the global transition to lower carbon economies.¹⁴ Therefore, developing technologies that enhance the portfolio of products derived from methane will help to alleviate our reliance on oil for chemical production.

The direct conversion of methane to chemicals has three main areas of interest 1) methane to ethylene, 2) methane to aromatics and 3) methane to methanol (Figure 2).¹⁵ Substantial progress has been made in all three areas however it is probably methane to ethylene that shows the greatest promise of a commercial process given recent announcements from Siluria Technologies that they have been running a pilot facility in La Porte, Texas since 2015¹⁶ and have recently executed a multi-plant technology license with Saudi Aramco to deploy the technology at existing sites.¹⁷

However it is direct methane to methanol (dMtM) that has been described as the holy grail of catalysis,¹⁸ and has been intensely tackled by both homogeneous and heterogeneous catalyst researchers. Perhaps what makes dMtM so tantalising is the very fact that nature has already been able to master this challenging chemistry in the form of methanotropic bacteria. These bacteria contain an enzyme, methane monooxygenase (MMO), which is capable of converting methane to methanol at physiological conditions.¹⁹ Two types of MMO enzymes exist, so called *particulate* and *soluble* forms, pMMO and sMMO respectively. The sMMO enzyme contains a dinuclear Fe centre in the active site while pMMO contains Cu.²⁰ The proposed structures of these active sites have inspired much research to develop laboratory mimics and have been a significant source of inspiration in the development of catalysts for dMtM.

The interest in dMtM shows no sign of waning. A number of excellent reviews have been recently published which cover dMtM,^{15, 19, 21-31} adding to the classic reviews in the field.³²⁻³⁷ Additionally, two opinion pieces proposing methods of overcoming poor reaction selectivity have very recently been written,^{38, 39} as well as modelling studies detailing optimal temperature and feed compositions for direct methanol production.⁴⁰ These articles highlight the collective desire to find a breakthrough that would bring dMtM technology closer to commercialisation.

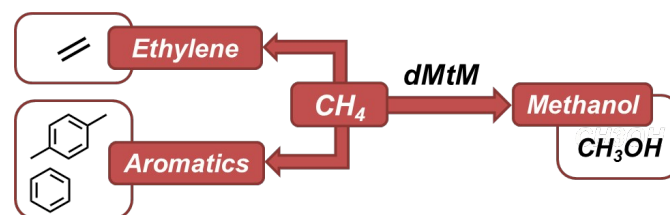


Figure 2: Schematic showing major products of the direct conversion of methane.

1.1 Brief history of dMtM

Since the beginning of the 20th century efforts to effect dMtM have been recorded. Articles in 1902 and 1903 reported on gas phase (homogeneous) partial oxidation of methane^{8, 41} while one of the first dMtM patents dates from 1905 when Lance and Elworthy described the synthesis of methanol by oxidizing methane with hydrogen peroxide in the presence of ferrous sulphate.⁴² Although efforts to effect dMtM over heterogeneous catalysts were reported in 1928,⁴³ the vast majority of subsequent research focussed on dMtM through partial combustion/oxidation in the absence of an added heterogeneous catalyst. However, by the 1960s a range of different supported metals had been identified as competent for dMtM.³¹ In 1969, Shilov reported that when methane was heated to 100 °C in a sealed ampoule containing PtCl₄ and a D₂O/CH₃COOD mixture, H/D exchange was observed to occur, indicating that methane activation could occur under mild conditions with a homogeneous catalyst.⁴⁴ This was the birth of so-called Shilov chemistry and resulted in the first example of direct methane to methanol by homogeneous platinum complexes under remarkably mild conditions (120 °C, in water).⁴⁵ Mechanistic studies of the Shilov system elucidated the key steps involved³⁰ and numerous efforts have been made to improve the system by ligation (see key reviews by Tilset³⁴ and others^{25, 29}). However, it has not been possible to bring the aqueous Shilov system close to commercial levels.

While not a direct conversion process, an important breakthrough in methane conversion came in 1998, with the report from Catalytica which utilised a ligand modified Pt system in fuming sulfuric acid to oxidise methane to methane bisulfate (Figure 3).^{46, 47} The system gave a single pass yield of

72% for methane bisulfate. Subsequent hydrolysis of methane bisulfate to methanol gave an overall selectivity of 81%.⁴⁸ More recently, Schüth has shown that the Catalytica system can be substantially improved upon by controlling the level of SO₃ in the oleum used and by using K₂PtCl₄ as a catalyst precursor in the absence of additional ligands.^{48, 49} The improvements led to turnover frequencies (TOFs) three orders of magnitude higher than the original system, giving process parameters which the authors showed are comparable to industrial processes such as the Cativa™ process (methanol carbonylation to acetic acid). However challenges remain in separating methane bisulfate from the reaction mixture and recycling the SO₂ by-product.⁴⁸ Furthermore, the inventory of oleum required may be off-putting, though it should be noted that refinery alkylation processes often use concentrated sulfuric acid on very large scales.⁵⁰ Although methanol is not produced directly, it is this exact feature of the reaction which prevents over oxidation, giving very high selectivities. This is a result of the methane bisulfate being deactivated with respect to further Pt mediated, electrophilic C–H activation due to the electron withdrawing effect of the sulphate group.

It is unsurprising to note that substantial heterogeneous catalysis research on dMtM has been conducted over early transition metal oxides, which find much use as oxidation catalysts through Mars-van Krevelen type mechanisms.⁵¹ In particular, the commercial production of maleic anhydride *via* partial oxidation of either benzene or n-butane has utilised oxides of molybdenum or vanadium as catalysts.⁵² Correspondingly, both vanadium oxide as well as molybdenum oxide catalysts have been studied for dMtM. Interestingly, catalysts based on MoO₃ and V₂O₅ can also form substantial quantities of formaldehyde during the process.⁵³⁻⁵⁵ By the late 1980s heterogenised molybdenum catalysts were some of the most active materials available for the dMtM reaction.⁵⁶⁻⁵⁸ In 2008 very impressive methane conversion and methanol selectivity values (13.2% and 78.8% respectively) were reported over an Fe/SiO₂ catalyst.⁵⁹ Mössbauer spectroscopic analysis of the catalyst indicated that 81% of the iron is present as supported hematite (Fe₂O₃), while 19% of the iron is embedded into the silica matrix as tetrahedral, Fe³⁺ sites.⁵⁹ No further articles on the system have been reported, but these impressive results over Fe/SiO₂ highlight the continuing improvements that are being made using heterogeneous catalyst systems.

By 1990 and beyond, metal-modified zeolites were being reported for the catalytic, direct partial oxidation of methane to methanol with molecular oxygen under flow conditions.^{60, 61} These pioneering results showed that methanol could be formed selectively under the right conditions. For example, the selectivity reported by Lyons *et al.* was 64% at 4.6% conversion⁶⁰ while Walsh reported 20.6 % selectivity at 5.5% conversion.⁶¹ However, it should be noted that as early as 1970, metal impregnated zeolites were reported as oxidation catalysts for toluene and xylene in the presence of air.⁶² These initial catalytic dMtM studies did not ascertain the nature of the active site but did show that enhanced MeOH yield and selectivity was attainable over such materials (by comparison

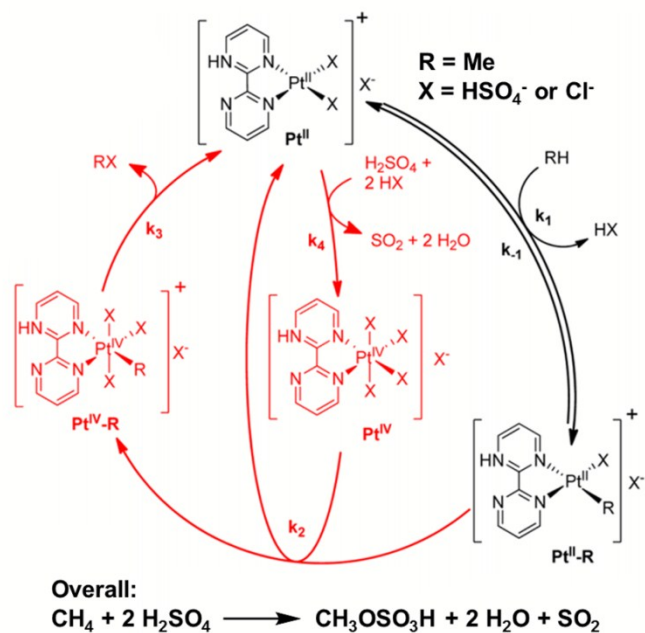


Figure 3: Proposed mechanism for the functionalisation of methane using (bpym)Pt(TFA)₂ in H₂SO₄ in the Catalytica system. Adapted with permission from reference 46. Copyright 2014 American Chemical Society

Walsh reported 47% selectivity at 0.2% conversion over glass beads).⁶¹ In 1995 Panov showed that methanol could be formed from methane by contact with the so-called α -Fe site, supported on ZSM-5.⁶³ The active site was at this stage unknown. However, the selectivity, after aqueous extraction, was shown to be 75%. This inspired others to further study these stoichiometric reactions in a bid to uncover the mechanism and active site requirements such that the yield and selectivity of the catalytic reaction may be improved. However, as studies have focussed on improving selectivity and mechanistic understanding, the number of studies concerning dMtM catalysis in flow has reduced dramatically. This could be considered detrimental to the industrialisation of dMtM as utilising a cyclical, multistep (and often non-isothermal) approach is less attractive than a continuous flow option, primarily as a multistep process is more complex and has lower thermal efficiency, and therefore a lower economic viability than a continuous flow process.

For a fuller account of the history of the dMtM reaction readers should look at the excellent review by van Bokhoven *et al.*³¹

Despite the progress in heterogeneous and homogeneous systems towards direct (and indirect) methane conversion to methanol, no system has yet been commercialised. This is indicative of the substantial hurdles that remain. In his 2015 article evaluating a dMtM production plant using current catalyst technologies, de Klerk highlights the areas where improvements need to be made in order to challenge the practiced syngas based route.⁶⁴ These areas are namely in improving MeOH selectivity/reducing CO₂ selectivity, reducing the need for pure oxygen (which introduces an air fractionation step) as well as keeping the reaction pressure to a minimum to reduce the compressor duty. We note that these areas can all be tackled by catalyst understanding and improvement, and serve as the basis for focus areas for further research. We also note that where methane is a by-product and simply flared it will not be necessary to benchmark against existing syngas based technologies.

1.2 dMtM by metal-modified zeolites

Zeolites are already extensively utilised for refinery and petrochemical processes⁶⁵ and are also well known to be able to induce reaction selectivities which differ to those predicted on thermodynamics alone. This can be achieved through the well-known *reactant, product and transition state selectivity*.⁶⁶ Additionally zeolites can impart remarkable reaction selectivity through *confinement*, where the free energy of the transition state is lowered by interactions with the framework, commonly van der Waals interactions and charge stabilisation by anionic T-sites.⁶⁷ The capacity to alter reaction selectivities through subtle substrate-framework interactions has drawn parallels with enzymes,⁶⁸ exemplified by the carbonylation of dimethyl ether to methyl acetate, which has been shown to selectively take place in the 8 membered ring (MR) side pockets of MOR.^{69, 70} Given that zeolites are already made and utilised on industrial scales, and demonstrate a remarkable

capacity to control reaction selectivity, it is fair to say that zeolite based catalysts have the potential to be industrial catalysts for dMtM. Subsequently, since Panov reported the highly selective conversion of methane to methanol over iron-modified ZSM-5 (Fe/ZSM-5),⁶³ although not catalytic, the field has grown enormously to become one of the most promising approaches to dMtM. This perspective focuses on the direct conversion of methane to methanol with first row d-block metal-modified zeolites, and in particular it examines the role of the extraframework metal and zeolite framework type in the reaction. The perspective will conclude by proposing new areas of research which the authors believe will be of benefit to the field. It should be made clear from the outset that when discussing dMtM in the context of zeolites the reactions are often non-catalytic, i.e. substoichiometric reactions, and performed in a multi-step process. In the main body of the text we shall predominantly consider reactions that utilise dioxygen as the source of oxygen as it is the preferred oxygen source for commercialisation. Where appropriate, comparisons may be made to other direct methane conversion reactions over zeolites.

2. Metal-modified Zeolites for dMtM

2.1 Fe-modified zeolites

Perhaps the most historic system within this field, Fe-modified zeolites have been known to be active in the oxidation of methane since the pioneering work of Panov *et al.* in the early 1990s.⁷¹ Early reports concluded that Fe/ZSM-5 is able to efficiently decompose N₂O at relatively low temperatures (< 300 °C) resulting in a highly reactive iron/oxygen species bound to the zeolite surface, termed α -oxygen (α -O) which is active for the direct partial oxidation of benzene to phenol at ambient temperature,⁷¹⁻⁷³ and was later deduced to be the active species in direct partial oxidation of methane to methanol. The formation of α -O is found to possess first order kinetics with respect to N₂O and cannot be formed by reaction with O₂ or NO.

Due to the presence of inactive spectator iron species, the nature of the active site and factors determining reactivity have been difficult to prove spectroscopically. Originally it was thought that the active precursor associated with the decomposition of N₂O (known as α -Fe) was a binuclear iron species, similar to that observed in MMO enzymes.⁷⁴ However, the α -Fe site was later determined to be a mononuclear Fe^{II} species formed *via* irreversible auto-reduction of impregnated Fe^{III} species upon thermal treatment.^{75, 76} A substantial contribution from Snyder *et al.* reports the use of magnetic circular dichroism (MCD) to elucidate significant structural and electronic information about both the α -Fe and α -O sites in zeolite beta (β).⁷⁶ It was found that α -Fe is a mononuclear, high spin Fe^{II} species residing within a square planar coordination environment. Further density functional theory (DFT) studies suggest that this square planar environment resides within a β -6MR (see Figure 4). Similarly, the α -O site is a mononuclear, high spin species which contains an Fe^{IV}=O

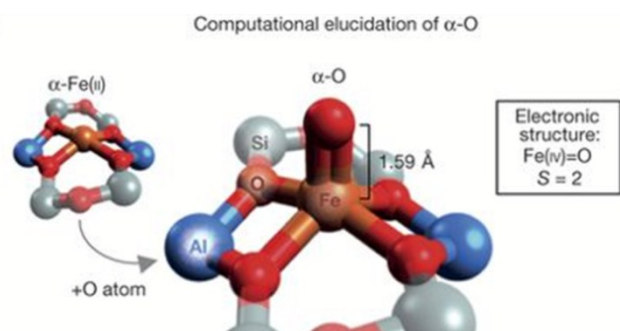


Figure 4: DFT-optimized structure of α -Fe(IV)=O in the $S=2$ ground state and its formation. Adapted with permission from reference 76. Copyright 2014 Nature 2016

centre adopting a square pyramidal geometry within the same β -6MR.

The general consensus regarding the methane-to-methanol reaction pathway over α -O sites is that it follows a radical based hydrogen atom abstraction mechanism, although steps following this are debated. Briefly, active α -O species are introduced into the catalyst by N_2O decomposition before methane is subsequently introduced. A hydrogen atom is abstracted from methane by the α -O resulting in an $Fe^{III}-O-H$ fragment and a CH_3 radical. This CH_3 radical may then either react with a further α -O to form $Fe^{III}-O-CH_3$ that may be extracted *via* hydrolysis or the CH_3 radical may 'rebound' to form an associated $Fe^{II}-O(H)-CH_3$ which may then desorb forming CH_3OH (Figure 5).^{75, 77} Formation of dimethyl ether (DME, CH_3OCH_3) has also been observed *via* the proposed reaction of a CH_3 radical with an already formed $Fe^{III}-O-CH_3$ group.⁷⁵ Kinetic isotope effect experiments suggest that initial C-H bond cleavage is the rate-limiting step in this process.⁷⁴ Fourier-transform infrared spectroscopy (FTIR) further supports the presence of the hydrogen atom abstraction process with computational evidence strongly suggesting that the C-H cleavage is performed *via* a radical mechanism with the $Fe^{IV}=O$ species elongating and gaining significant radical character at the transition state, becoming closer to an $Fe^{III}-O^*$ species.^{75, 76}

The remarkable activity of the α -O site is partially attributed to confinement effects within the zeolite channels.^{52, 77} Periodic and cluster modelling of an α -O site in SSZ-13 have shown that the confining effect of zeolite channels may reduce the energetic barrier to methane activation by over 50%.⁷⁷ It is suggested that the confinement effect is predominantly electrostatic in nature and stabilises reaction intermediates and transition states to a further degree than that of the initially adsorbed methane molecule.⁷⁷ The key effect is stated to be the stabilisation of the intermediate species, suggesting that tighter confinement leads to lowered C-H bond activation energy owing to a Brønsted-Evans-Polanyi relationship.

In order to become more viable at large-scale, the requirement for batch-style oxidative pre-treatments and liquid phase extraction should be avoided. Hence, several attempts have been made to produce methanol from methane over Fe-modified zeolites under a continuous or catalytic

regime, although success has been limited. The reaction has been reported to occur in a "quasi-catalytic" manner at 160 °C over Fe/ZSM-5 under an atmosphere of $CH_4:N_2O$ with stoichiometry of 1:1 and single site turnover number (TON) of 3.6, although liquid phase extraction of products was still required.⁷⁸ The >1 TON is attributed to methanol spill over, suggesting that methoxy species can migrate within the framework, reforming the α -Fe site and allowing another catalytic cycle to take place. It is suggested that the reaction temperature (160 °C) is insufficient to promote methanol desorption. A later contribution describes the continuous flow reaction of N_2O and CH_4 over Fe/ZSM-5 at 300 °C.⁷⁹ Methanol was observed with only very low selectivity (ca. 1%) while CO is observed as the major product. This is attributed to the inability of methanol to desorb from the catalyst, instead migrating to nearby Brønsted acid sites and rapidly producing coke in subsequent reactions akin to those seen in the methanol-to-olefins process. Upon introduction of water in a co-feed, the selectivity to methanol is seen to greatly improve, reaching around 16%. It is thought that the additional water hydrolyses adsorbed methanol and methoxy species, allowing them to leave the catalyst, a hypothesis that is concordant with an observed decrease in coke formation. Activation of N_2O by extra-framework iron species is not experimentally limited to MFI framework types alone with evidence for N_2O decomposition over MOR, FER and FAU having been reported.⁸⁰⁻⁸³ In each case it has been shown that framework oxygen atoms are able to be isotopically exchanged with $N_2^{18}O$. N_2O decomposition and subsequent methane activation have also recently been observed to take place on both Fe/BEA and Fe/CHA, resulting in the production of methanol which was able to be recovered by liquid extraction.^{76, 84} From computational studies, it is found that in the CHA case the α -O site is also stabilised within a 6MR, similar to that of BEA but with subtle differences in their geometries. The mononuclearity of the CHA α -O site was confirmed by Mössbauer spectroscopy.⁸¹ Ferrisilicate, a zeolite material containing only Si and Fe tetrahedral atoms and adopting an MFI framework type, has been shown to be active in the direct conversion of methane to methanol using O_2 as an oxidant as opposed to N_2O .⁸⁵ This is of significant interest as α -O sites in aluminosilicates are unable to form from O_2 , always requiring N_2O instead. In contrast to Fe-modified aluminosilicate systems which are able to activate methane and form methanol at ambient temperatures, the ferrisilicate systems require much greater temperatures (350 °C) for reaction to take place although the observed methane conversion at this temperature is only around 0.1%. Temperatures even higher still (630 °C) are needed for substantial methane conversion to be observed where methane conversions up to around 30% are seen, although at significant cost of methanol selectivity. The requirement for much higher temperatures to achieve even low-level conversion coupled with the ability to utilise dioxygen as an oxidiser strongly suggest that the ferrisilicates system contains an active site different to that of Fe-modified aluminosilicate zeolites. No mechanism has been suggested as to how this

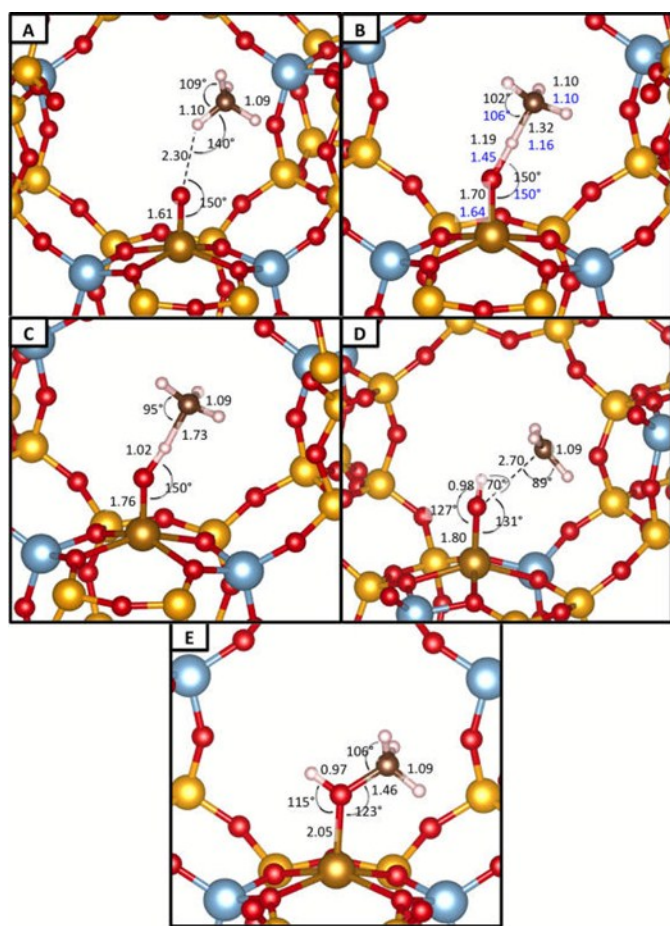


Figure 5: Structures and the most important intermediates (adsorbed molecule (A), reaction intermediate (C), and adsorbed methanol (E)) and transition states (abstraction transition state (B) and rebound transition state (D)) along the reaction pathway of dMtM over the α -O site. Colour legend: Si atoms, yellow; O atoms, red; Al atoms, blue-grey; Fe atoms, gold; H atoms, white; and C atoms, brown. Black numbers represent PBE-D2 distances (in Å) and angles (in degrees); blue numbers in panel (B) show the optimized RPA geometry. Adapted with permission from reference 77. Copyright 2016 American Chemical Society

transformation takes place over ferrisilicates and hence a mechanistic comparison with respect to the α -O site cannot be made as yet. For the ferrisilicates system, a higher Si/Fe ratio was shown to result in higher methanol selectivity, although at the expense of percentage methane conversion. Both H- and Na-form ferrisilicates were compared, with Na-forms demonstrating higher selectivity for methanol.

In addition to gaseous phase activation by O_2 or N_2O , several recent contributions have investigated the use of an aqueous phase oxidant, H_2O_2 , in the dMtM reaction over Fe-modified zeolites.⁸⁶⁻⁹⁰ In contrast to what has been highlighted previously, this system is not thought to proceed *via* α -O formation (Fe^{II}/N_2O system) but instead by a mechanism that utilises extra-framework Fe^{III} oxides, intermediately forming methyl hydroperoxide (CH_3-OOH) which is subsequently transformed into the desired methanol product alongside further oxidised products, namely formic acid and carbon oxides.⁸⁷

The initially reported system demonstrated that hydrothermally synthesised Fe-silicalite-1 (0.5 wt% Fe) was able to transform methane into various C_1 oxygenates with a selectivity of 94% at 0.3% conversion within 30 minutes. In terms of oxygenate distribution, 17% of the total selectivity was to the desired methanol product whilst the remaining product was predominantly formic acid.⁸⁶ The reaction was carried out in an autoclave under the following conditions: 27 mg of the desired catalyst was stirred in 10 mL of 0.5 M H_2O_2 under a 30.5 bar pressure of CH_4 for 30 minutes at 50 °C. Interestingly, even commercial ZSM-5 containing only trace amounts of Fe (0.014 wt%) was found to be comparably active, achieving 95% total oxygenate selectivity at 0.3% conversion with a similar product distribution. Non-modified silicalite-1 (0 wt% Fe), however, was found to be inactive, achieving 0% conversion under the same reaction conditions. The implication of these results is that at least a low level of framework Fe is required to achieve activity under the employed reaction conditions.

In order to elucidate the role that Fe speciation plays within the catalytic process and to determine whether framework or extra-framework Fe species were the active sites, the nature of the Fe active sites was thoroughly investigated in further reports.^{88, 89} Although FT-IR, UV-Vis and porosimetry methods demonstrate that the "as-prepared" Fe-silicalite-1 is shown to possess predominantly framework Fe species,⁸⁸ it is thought that the active species for methane oxidation is actually extra-framework oligomeric Fe oxide species resulting from high temperature thermal treatment. Upon various thermal treatment temperatures (550, 750, 950 °C) it was observed in the associated UV-Vis spectra that the absorbances corresponding to framework Fe species decrease upon increasing pre-treatment temperature whilst those resulting from oligomeric and higher extra-framework Fe species increase, suggesting that Fe species are removed from the framework to some degree. The authors suggest that catalytic activity is associated with small oligomeric extra-framework Fe species located within the zeolite micropores. The percentage of Fe species that are oligomeric in nature increases with increasing pre-treatment temperature and a maximum was observed following pre-treatment at 750 °C; treatment at 950 °C was shown to produce fewer oligomeric Fe species and larger Fe clusters and bulk Fe oxides. This data correlates well with catalytic tests which demonstrate that higher temperature pre-treatments result in higher yields of oxygenated products, reaching a maximum at 750 °C and dropping again following pre-treatment at 950 °C.⁸⁸ It has been further reported that the presence of other trivalent cations (Al^{3+} , Ga^{3+}) within the system prior to pre-treatment, whilst not constituting catalytically active centres, facilitate Fe removal from the framework and hence increase the formation of active extra-framework Fe species.⁸⁹

It was further demonstrated that addition of Cu^{II} species to the previously described hydrothermally synthesised Fe-silicalite-1 can have a dramatic effect on partial oxygenate selectivity.^{86, 87} When Cu^{II} was introduced to commercial ZSM-5 (0.014 wt% Fe) by solid-state ion exchange (SSIE), the

conversion was seen to remain constant when compared to the unmodified catalyst whereas the selectivity to methanol was seen to increase dramatically from 19% to 83% under the same reaction conditions.⁸⁶ Even the introduction of aqueous $\text{Cu}^{\text{II}}(\text{NO}_3)_2$ (10 μmol Cu) to a previously tested system was seen to drastically increase methanol selectivity when compared to the original material at very similar conversions. In contrast, SSIE introduced Cu/silicalite-1 (0 wt% Fe) was seen to be inactive for the conversion of methane under the reaction conditions. This led the authors to conclude that, while Cu^{II} species are not able to perform methane partial oxidation, they are active in preserving the formed methanol and preventing over-oxidation to formic acid and carbon oxides.⁸⁷ Under optimised reaction conditions (54 mg catalyst, 20 mL, 1.0 M H_2O_2 , $P(\text{CH}_4) = 3$ bar, 30 minutes, 70 °C), Fe-silicalite-1 (0.5 wt% Fe) was seen to produce 8% methanol at 10.5% conversion whilst a bicatalytic system containing Fe-silicalite-1 and SSIE introduced Cu/silicalite-1 was seen to demonstrate a methanol selectivity of 93% at 10.1% conversion.⁸⁶ Additionally, the $\text{H}_2\text{O}_2/\text{FeCu-ZSM-5}$ system has recently been tested in a continuous flow regime under optimised conditions of: 1.5 g catalyst, $P(\text{CH}_4)$ 20 bar, Flow (CH_4) = 10 mL min^{-1} , Flow (H_2O_2 , 0.123 M) = 0.25 mL min^{-1} , 50 °C.⁹⁰ In this regime it was observed that high methanol selectivity was able to be retained (92 %) at a conversion of 0.5%.

Overall, the active sites ($\alpha\text{-Fe}$ and $\alpha\text{-O}$) in Fe-modified zeolite systems have been well characterised, whereas the mechanism of C–O bond formation following initial hydrogen abstraction requires further elucidation. Although a well-established system, potential for exploration of methanol production over different framework types and expansion to continuous flow processes is ripe. A major factor determining the success of Fe-modified zeolite systems will be the ability to use O_2 as an oxidant as opposed to N_2O , which, owing to its energetic nature, is generally undesirable for large-scale industrial usage. In this regard, investigation of methane partial oxidation over ferrisilicates holds promise within this area.

2.2 Cu-modified zeolites

Since the first report of methane partial oxidation to methanol over copper-modified zeolites in 2005, the field has been subject to intense scientific interest and research.⁹¹ Methanol formation has since been shown to be possible over a wide range of copper-modified zeolite frameworks including: MFI, MOR, FER, CHA, FAU, BEA, LTL, EON, MAZ, MEI, BPH, HEU, SZR, AFX and AEI.⁹²⁻⁹⁴ Within these frameworks, a wide variety of active sites have been proposed for this important transformation.

2.2.1 Active sites for methane partial oxidation in copper-modified zeolites

Unlike iron-modified zeolites in which it is thought that only one site (the so-called $\alpha\text{-Fe}$ site) is active for methane partial oxidation to methanol, there have been multiple active sites proposed to exist in copper-modified zeolites. The first

site to be proposed for methane C–H bond activation in Cu/ZSM-5 was the bis($\mu\text{-oxo}$)dicopper core (Figure 6A) that had previously been identified for the decomposition of NO ⁹⁵ and was thought to be characterised by a strong absorption band at 22700 cm^{-1} in the ultraviolet-visible-near infrared (UV-Vis-NIR) spectrum.⁹¹ Another active site, a ($\mu\text{-}\eta^2\text{:}\eta^2\text{-peroxo}$)dicopper core (Figure 6B) which is active in nature for O_2 transport by the protein hemocyanin, was also suggested, but was not observed to be active in NO reduction.^{91, 95, 96}

A considerable contribution by Woertink *et al.* utilised resonance enhanced Raman spectroscopy (rR) to further elucidate the active site structure in Cu/ZSM-5.⁹⁷ By tuning a laser to the characteristic absorption feature identified with the active site (22700 cm^{-1}), the Raman vibrations associated with this feature are enhanced, enabling the ~5% active species to be distinguished from spectator Cu. As a result, the bis($\mu\text{-oxo}$)dicopper and ($\mu\text{-}\eta^2\text{:}\eta^2\text{-peroxo}$)dicopper cores were able to be discounted due to inconsistencies with the observed rR stretching frequencies. Instead, a bent mono($\mu\text{-oxo}$)dicopper core (Figure 6C) was proposed as the active site owing to a series of isotope-sensitive fundamental vibrations at 456 cm^{-1} ($\Delta^{18}\text{O}_2 = 8 \text{ cm}^{-1}$) and 870 cm^{-1} ($\Delta^{18}\text{O}_2 = 40 \text{ cm}^{-1}$) alongside an intense overtone of the latter at 1725 cm^{-1} ($\Delta^{18}\text{O}_2 = 83 \text{ cm}^{-1}$). This intensity pattern closely resembles that seen for mono($\mu\text{-oxo}$)diferric cores.^{97, 98} The mono($\mu\text{-oxo}$)dicopper species is suggested to exist within the 10MR channel of ZSM-5, bridging two framework aluminium sites separated by two silica tetrahedra. Each copper atom of the mono($\mu\text{-oxo}$)dicopper core is ligated by two oxygen atoms associated with the framework aluminium alongside the bridging oxygen. Normal co-ordinate analysis predicts a Cu–O–Cu bridging angle of 140°. The copper species are proposed to be formally Cu(II), as Cu(III) cannot be stabilised without co-ordination of a further –OH group of which no evidence was detected by rR spectroscopy.⁹⁷

The mono($\mu\text{-oxo}$)dicopper core can be formed by activation in both N_2O and O_2 as evidenced by observation of the UV-Vis-NIR band at 22700 cm^{-1} that is associated with this active site.^{99, 100} Activation by N_2O can occur at room temperature by liberation of N_2 with the lowest energy pathway for N–O cleavage — the oxygen bridging mode ($\mu\text{-}1,1\text{-O}$).¹⁰¹ Activation by O_2 proceeds at room temperature *via* the

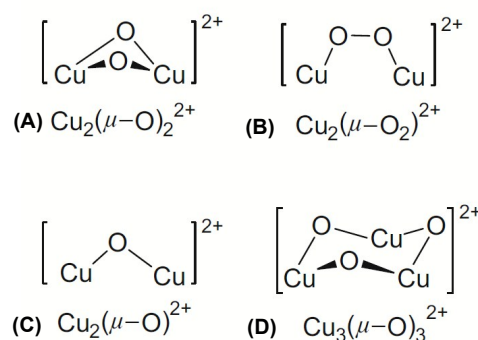


Figure 6: Cu-oxo complexes proposed as the active sites for methane activation in Cu-containing high-silica zeolites. Adapted with permission from reference 122. Copyright 2016 Elsevier

formation of a $(\mu-\eta^2:\eta^2\text{-peroxo})$ dicopper core which can be characterised by a strong UV-Vis-NIR absorption band at 29000 cm^{-1} .¹⁰⁰ Heat treatment in flowing He or O_2 results in the decrease of the 29000 cm^{-1} band and a coincidental increase of the 22700 cm^{-1} band from approximately 448 K, demonstrating formation of the mono(μ -oxo)dicopper core (Figure 7). This conversion results in the deposition of an oxygen atom on other remote Cu sites within the zeolite as evidenced by $^{18}\text{O}_2$ TPD.¹⁰⁰ It has been further proposed that spectator Cu^+ ions in ion exchange sites provide the necessary electrons to reduce the peroxo-bridge.¹⁰⁰

Larger copper clusters have been both evidenced and predicted as active sites for the partial oxidation of methane in copper-modified zeolite systems. A trinuclear copper core, $[\text{Cu}_3(\mu\text{O})_3]^{2+}$, has recently been proposed to exist at the mouth of the 8MR side pocket of Cu/MOR (Figure 6D).¹⁰² Extended X-ray absorption fine structure (EXAFS) measurements suggest that more than one Cu-Cu scattering path exists within the cluster, suggesting a nuclearity >2 . From investigations into the change in acidity of the zeolite upon active site formation, it was shown that two Brønsted acid sites are displaced for every three Cu atoms incorporated into the structure. As a result, it is suggested that the trinuclear cluster is balanced between two aluminium atoms, each separated by three silica tetrahedra.

DFT simulations of mono(μ -oxo)dicopper and $[\text{Cu}_3(\mu\text{O})_3]^{2+}$ cores in Cu/ZSM-5 have shown that under standard activation protocols (high temperature calcination in O_2) the trinuclear species is more stable than the binuclear species, whereas the binuclear species is preferentially formed under low partial pressures of O_2 .¹⁰³ Previously identified binuclear and trinuclear cores alongside clusters of higher nuclearity ($[\text{Cu}_n\text{O}_{n-1}]^{2+}$ and $[\text{Cu}_n(\mu\text{O})_n]^{2+}$, where $n = 2, 3, 4, 5$) in Cu/MOR have also been simulated by DFT calculations in order to compare their stability and reactivity.¹⁰⁴ It was found that as the cluster increases in size, it becomes both more stable as a cluster and that increased reactivity with methane is strongly correlated with this increased stability.

In small pore zeolites such as CHA, several potential

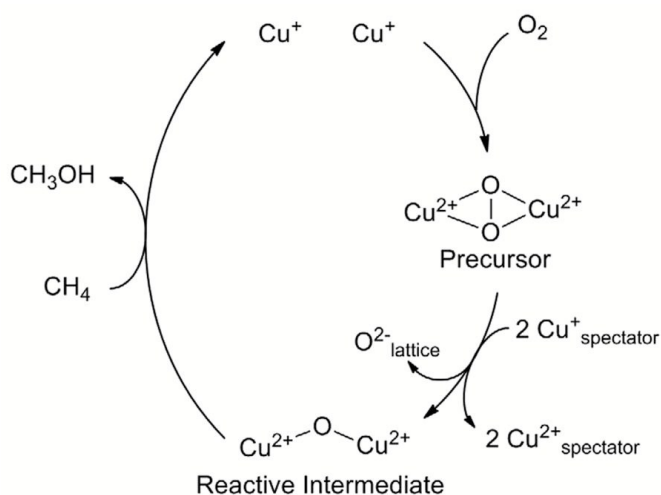


Figure 7: Formation of the mono(μ -oxo)dicopper core in the presence of O_2 . Adapted with permission from reference 100. Copyright 2010 American Chemical Society

mononuclear extra-framework Cu cations have been identified both experimentally⁴⁰ and using DFT calculations.^{105, 106} Specifically, $[\text{CuOH}]^+$ has been suggested to be active for methane partial oxidation in Cu/SSZ-13 and is predicted to be stabilised within an 8MR CHA that contains only one charged aluminium species.^{105, 106} This species is believed to be formed upon dehydration of hydrated Cu^{2+} species and is characterised by a FTIR stretch at $\nu(\text{O-H}) = 3657\text{ cm}^{-1}$.^{107, 108}

2.2.2 Reaction mechanism for the partial oxidation of methane over copper-modified zeolites

Typically, methane partial oxidation over copper-modified zeolites is observed to take place in three distinct steps. Initially, the copper-exchanged zeolite is activated in an oxidative atmosphere using either O_2 , at elevated temperature (typically 723–823 K), or N_2O , at from as low as room temperature.^{91, 109, 110} The activated material is then exposed to methane at a moderate temperature (approx. 473 K) followed by subsequent extraction of the strongly bound products through contact with water vapour or a suitable solvent, such as a 1:1 mixture of acetonitrile and water.^{22, 91}

Thus far, methane activation over copper-modified zeolites has only been proposed to occur *via* a radical type mechanism with DFT calculations having proved crucial for elucidation of this mechanism and kinetic isotope experiments proving important for determination of the rate-limiting step.^{97, 103, 110, 111} The mono(μ -oxo)dicopper core, formally denoted as $\text{Cu}^{2+}-\text{O}^{2-}-\text{Cu}^{2+}$, is thought to be in resonance with what is effectively a cupric-oxyl species, $\text{Cu}^{2+}-\text{O}^{\bullet}-\text{Cu}^+$ (Figure 8), which possesses significant radical character owing to its singly occupied molecular orbital (SOMO) that is directed into the zeolite channel.^{97, 103} This resonance form is aptly poised to perform hydrogen atom abstraction from methane to form an intermediate Cu-OH-Cu species and a CH_3 radical. This preliminary step shows a considerable H/D kinetic isotope effect of 3.1 at 448 K when the activation energies of CH_4 and CD_4 are compared.⁹⁷ This has been further confirmed when the products of a mixed substrate (CH_2D_2) were reacted over Cu/ZSM-5 at 403 K (as analysed by ^1H NMR spectroscopy, following extraction into D_2O).⁹⁷ In this analysis, a greater product integral is observed for CD_2HOD than for CDH_2OD implying that the rate of C-H cleavage is greater than that of the C-D bond. In a separate study an H/D KIE of 1.6 was determined when CH_4 was substituted by CD_4 in the extracting gas at 483 K over Cu/Na-ZSM-5.¹⁰⁹ These observations alongside DFT predictions show that hydrogen abstraction is the rate limiting step in methanol formation from methane.

The newly formed “free” CH_3 radical intermediate has been predicted to collapse in several ways to form bound intermediates of various stability.¹⁰³ Two potential pathways can lead to the formation of a strongly bound, yet desired, methanol molecule (Figure 9). The first pathway is known as the “rebound mechanism” in which the CH_3 radical reacts directly with the bridging Cu-OH-Cu and forms a sorbed methanol molecule, $\text{Cu}-(\text{CH}_3)\text{OH}-\text{Cu}$. It is also possible that the CH_3 radical reacts with one of the copper atoms before migrating to the bridging oxygen atom; this pathway proceeds

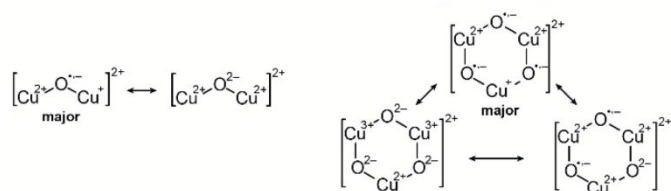


Figure 8: Possible resonance structures that could be proposed to describe the formal charge configuration in the extra-framework copper species. Adapted with permission from reference 103. Copyright 2016 Elsevier

via an intermediate $\text{CH}_3\text{-Cu-OH-Cu}$ species. However, the lowest energy pathway calculated proceeds via reaction between the CH_3 radical and framework oxygen atoms. This results in formation of a zeolite grafted methoxy group ($\text{CH}_3\text{-O}_{\text{FW}}$) and reduced copper cluster, $\text{Cu}^{\text{I}}\text{-O-Cu}^{\text{I}}$. The production of methanol from this state is predicted to be highly unlikely owing to the need to spontaneously reform the CH_3 radical.¹⁰³ It should be noted that alternative mechanistic intermediates have been proposed previously. Prior reports utilised DFT calculations to predict formation of both Cu-OH-Cu and $\text{Cu-OCH}_3\text{-Cu}$ species as stable intermediates upon hydrogen atom abstraction, resulting in an exothermic methane activation step as opposed to an endothermic step associated with $\text{Cu}(\text{CH}_3)\text{OH-Cu}$ formation.^{97, 112} Introduction of water vapour then allows desorption of the methoxy intermediate as methanol.

The mechanism of action for methanol production for the trinuclear $[\text{Cu}_3(\mu\text{O})_3]^{2+}$ core is predicted to occur in a similar fashion to the binuclear equivalent. Although formally identified as a mixed Cu(III)/Cu(II) species owing to the formal $\text{O}(-\text{II})$ charge of the bridging oxygen atoms, DFT, Bader charge and spin-polarized charge density calculations suggest that the trinuclear species is more aptly described as a radical species, similar to that seen for the binuclear equivalents.^{102, 103} Therefore this species is proposed to exist as a mixed Cu(II)/Cu(I) system possessing radical anionic oxygen ligands in resonance with the formally charged species and one other form (Figure 8).

The initial step of methane partial oxidation over $[\text{Cu}_3(\mu\text{O})_3]^{2+}$ remains to be H-atom abstraction, however, unlike the

binuclear mechanism, direct methanol formation (rebound mechanism) is thermodynamically strongly favoured over the formation of grafted, framework methoxy groups ($\text{CH}_3\text{-O}_{\text{FW}}$) and copper bound methyl species ($\text{CH}_3\text{-Cu-OH-Cu}$). The most energetically favoured pathway in this system, however, is the combination of the CH_3 radical with another μ -oxo bridge associated with the cluster. From this point, adsorbed methanol can be formed by intermolecular proton transfer (Figure 9).¹⁰³

Methane partial oxidation over mononuclear copper sites, $[\text{CuOH}]^+$, has also been predicted by DFT calculations to occur via a radical hydrogen atom abstraction pathway.¹⁰⁶ Initially in this pathway, a hydrogen atom is abstracted from methane to form a hydrated copper species and a CH_3 radical. The formed CH_3 radical may then directly insert into $[\text{Cu-OH}_2]^+$ to form a bound methanol molecule, although the calculated activation barrier to this transformation renders it unlikely. Formation of $[\text{CH}_3\text{-Cu-OH}_2]^+$, however, is facile. Experimentally, NIR spectroscopic analysis supports the latter pathway, providing evidence for the existence of a $[\text{CH}_3\text{-Cu-OH}_2]^+$ or $[\text{CH}_3\text{-Cu-OH}]^+$ intermediate.¹¹³

As the methanol produced is strongly adsorbed in all cases, co-adsorption of water is required to either hydrolyse the methoxy intermediate or desorb the formed methanol. It is not considered possible to thermally desorb methanol as increased reaction temperatures may result in further oxidation to CO_2 . Following removal of products, it is possible to regenerate both binuclear and trinuclear copper species by reactivation in O_2 , hence the reaction pathway may be described as a stepwise cycle as opposed to continuous. In the case of the trimeric active site, $[\text{Cu}_3(\mu\text{-O}_3)]^{2+}$, DFT calculations predict that a second C-H activation reaction may occur prior to regeneration of $[\text{Cu}_3(\mu\text{-O}_2)]^{2+}$ proceeding via an analogous pathway that is similar energetically to the first reaction.¹¹⁴

2.2.3 Alternatives to stepwise methanol production: Isothermal and direct catalytic conversion of methane to methanol over copper-modified zeolites

As previously stated, most systems that convert methane to methanol over copper-modified zeolites occur in three

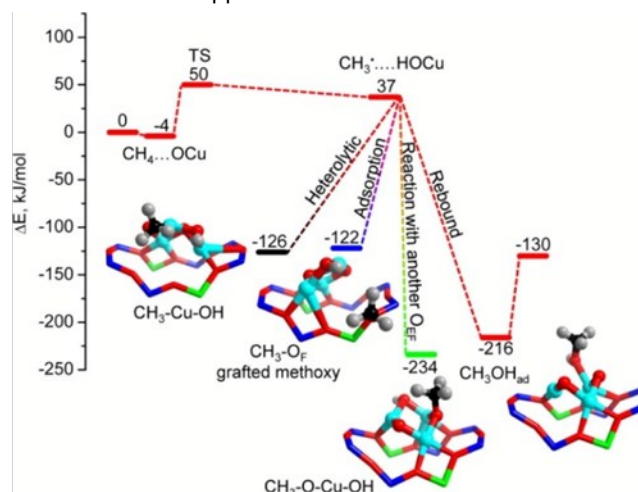
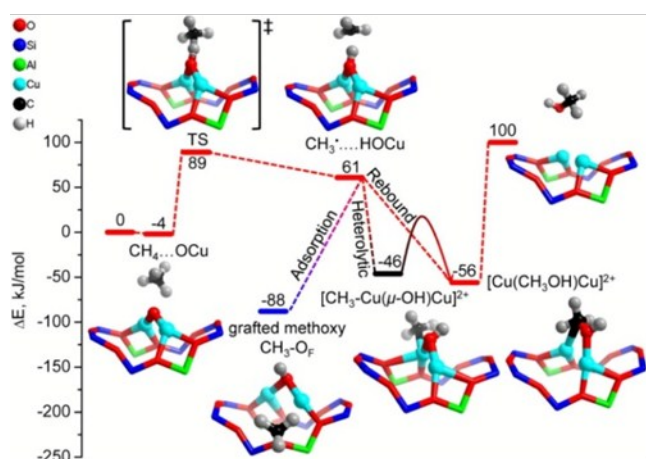


Figure 9: Reaction pathways for methane oxidation to methanol, and alternative CH_3 recombination routes over binuclear $[\text{Cu}_2(\mu\text{O})]^{2+}$ (left) and trinuclear $[\text{Cu}_3(\mu\text{O})_3]^{2+}$ (right) sites. Adapted with permission from reference 103. Copyright 2016 Elsevier

distinct steps that are performed over a variable temperature range. This represents a significant barrier to commercial exploitation as substantial temperature changes lower both the production efficiency (time is wasted waiting for the reactor to heat or cool) and thermal efficiency (heat is wasted repeatedly heating and cooling the reactor) of the process, hence resulting in reduced profitability.¹¹⁵ Several recent reports, however, have shown the ability to run this reaction in an isothermal regime using O₂ or NO as an oxidant at 473 K and 423 K respectively.^{115, 116} Within this mode of operation, both activation and methane exposure steps are run at the same temperature. It is found in the case of isothermal activation with O₂ that methanol yield depends greatly on methane inlet pressure; increasing the inlet pressure from 50 mbar to 37 bar resulted in an increase of methanol yield per gram of catalyst of approximately two orders of magnitude (0.3 μmol g⁻¹ and 56.2 μmol g⁻¹ respectively). The dependence of methanol yield on methane partial pressure indicates that the active sites present are non-uniform in nature.¹¹⁵ This may be either due to the presence of additional active species (e.g. higher nuclearity clusters, as suggested by the authors),¹¹⁵ and/or potentially in the extraframework distribution of the clusters present (such as at channel intersections). It is also feasible that the specific distribution of framework aluminium sites can alter the active site potency as observed for Zn²⁺ sites in ZSM-5.¹¹⁷

Recent reports have suggested that certain active sites within copper-exchanged zeolites (specifically Cu/MOR) may be regenerated under step-wise isothermal “anaerobic” conditions, using water as a softer oxidant than O₂.¹¹⁸ Following initial high temperature activation under He (673 K), the temperature is lowered to 473 K for methane activation and subsequently water is used to concurrently desorb methanol whilst regenerating the active sites at the same temperature.¹¹⁸ Upon introduction of isotopically labelled water (H₂¹⁸O) into the step-wise reactor, the mass spectrum signal from unlabelled methanol (CH₃¹⁶OH) was seen to decrease whilst that from labelled methanol (CH₃¹⁸OH) increased, suggesting the incorporation of ¹⁸O within the active site of Cu/MOR.¹¹⁸ The suggested mechanism of action for this regeneration is the bridging co-ordination of water between the newly reduced Cu species, [Cu^I-OH₂-Cu^I], followed by re-oxidation and liberation of H₂, which was observed *via* mass spectrometry.¹¹⁸ Owing to the bridging nature of this intermediate, it is suggested that only oligomeric copper species (Cu nuclearity ≥ 2) may be regenerated under these anaerobic conditions.¹¹⁸ This work, however, has been the subject of strong debate within the associated community, with several technical comments and replies questioning and defending the thermodynamic feasibility of the proposed mechanism.¹¹⁸⁻¹²¹

The overarching objective of methane partial oxidation research, however, is to provide a system in which methanol can be produced in a catalytic fashion under continuous flow conditions using O₂ as an oxidant. At the time of writing, literature surrounding methanol production over copper-modified zeolites within a catalytic regime is relatively sparse,

yet promising none the less. A recent contribution reports testing of various copper-modified zeolite and silica frameworks for the production of methanol from methane using a feed gas mixture of CH₄/O₂/H₂O at moderate temperatures (483–498 K).¹⁰⁹ Methanol production values of approximately 0.30–3.12 μmol_{MeOH} g_{cat}⁻¹ h⁻¹ were observed over different frameworks and are suggested to be the result of various topologies better stabilising transition states and active sites. Isotopic pulsing by the introduction of ¹³CH₄ into the feed gas resulted in detection of a pulse of ¹³C enriched methanol (¹³CH₃OH) within the mass spectrum; similarly, isotopically enriched ¹³CO₂ was observed as a side product during a pulse. While a very valuable contribution to the field, major limitations of the catalytic system are apparent by the fact that approximately 300 hours of time on stream (TOS) were required to generate a cumulative 1.4 mol_{MeOH} mol_{Cu}⁻¹. Furthermore, the high selectivities reported for methanol formation are due to the limited concentration on oxygen in the feed (25 ppm) which clearly limited the maximum possible yield of methanol in order to prevent over-oxidation to carbon oxides.

2.2.4 Effect of framework topology and composition on methane partial oxidation over copper-modified zeolites

The varying topologies and compositions of copper-modified zeolites are thought to have a large effect on not only their ability to produce methanol, but also the nature of the active sites responsible. As a general observation, frameworks containing a higher Si/Al ratio in which the Al atoms are more dispersed are more likely to support monomeric active sites, whereas those with a lower Si/Al ratio are likely to have several Al atoms within close proximity that are able to stabilise multinuclear copper clusters.¹²¹ Thus far, ZSM-5 and MOR frameworks have been studied most intensively, although many small pore frameworks, such as SSZ-13, have recently been subject to intensified investigation.

2.2.4.1 ZSM-5 (MFI framework)

Although not as efficient as other copper-modified zeolites in terms of methanol production, Cu/ZSM-5 has been used to great extent to help characterise the active sites involved in methane partial oxidation, their formation and the reaction mechanism. Cu/ZSM-5 is suggested to host various active sites depending upon the Cu loading and Al distribution with the framework which can have a major effect on methanol production.¹²² The major active site within Cu/ZSM-5 is suggested to be the bent mono(μ-oxo)dicopper species, characterised by the UV-Vis-NIR band at 22700 cm⁻¹.⁸⁹ Evidence for the existence of trinuclear active species in Cu/ZSM-5 has been published recently;¹²² DFT calculations also predict that the trinuclear species is indeed more stable than the binuclear species in the MFI zeolite framework.¹⁰³ At particularly low Cu loadings (or in a zeolite with highly disperse Al atoms) multinuclear species cannot form and mononuclear species are formed instead, resulting in relatively low methane partial oxidation activity. As the loading of copper increases, it becomes more likely that two Cu atoms will be proximal enough to one another to condense and form a binuclear site

(providing there are sufficient Al atoms to stabilise it). Upon further increase in Cu loading, the same logic is applied and trinuclear species may form. Once all potential framework sites for cluster formation are occupied, monomeric Cu species may be exchanged onto isolated Al atoms and CuO_x may form.¹²² Cu exchanged onto the surface of ZSM-5 is thought to be in the form of CuO_x and inactive in methane partial oxidation.¹²³ There is an argument to be made, however, that the Cu species within the channel and at channel intersections reside in different local environments, and hence have differing reactivity towards methane partial oxidation.¹²²

2.2.4.2 Mordenite

Although ZSM-5 was the first zeolite framework to be investigated for dMtM, the vast majority of the research regarding methane partial oxidation over copper-modified zeolites has been performed with regard to Cu/MOR as it is typically observed to produce a higher methanol yield.⁹¹ At the 8MR windows of the side pockets, Cu/MOR has been suggested to possess both binuclear and trinuclear clusters capable of performing methane partial oxidation.^{91, 102} Recent spectroscopic observations¹²⁴ and DFT simulations¹¹⁴ have further suggested that Cu/MOR possesses two mono(μ -oxo)dicopper species predicted to be distinct with respect to their siting within the 8MR side pocket.¹¹⁴ The UV-Vis-IR band originally associated with a single activated Cu/MOR species at approximately 22000 cm^{-1} has instead been suggested to be comprised of two bands centred at 21900 cm^{-1} and 23100 cm^{-1} .¹²⁴ Interestingly, these two different sites demonstrate substantial reactivity differences despite very similar geometric and electronic structures. It was further noted that only one of the two active sites is stable above 603 K.¹²⁴ Very recently it has been reported that the two species observed are the result of confinement within the multidimensional structure of MOR.¹²⁵ Confinement of the $[\text{Cu}_2\text{O}]^{2+}$ dimer in the 8MR side pocket of MOR gives rise to a lower activation barrier as a result of stabilisation of the transition state through van der Waals contacts with the framework. This effect of confinement, sometimes known as the nest effect,¹²⁶ is substantially less well known than the other shape selective effects imparted by zeolite micropores. Interestingly, confinement in the 8MR side pockets of MOR has been shown to give rise to a remarkable increase in reaction rate, and therefore selectivity, in the carbonylation of carbon monoxide to form methyl acetate.^{69, 127} Additionally, the role of confinement within zeolites in a number of other catalytic systems has been recognised by the Iglesia group.^{67, 128, 129} The ability of confinement to selectively enhance the rate of one reaction over another through transition state stabilisation is an enticing mechanism by which to “break” the thermodynamic limitations on methane partial oxidation (or change the selectivity outcome of the partial oxidation of methane).

Owing to the amount of methanol extracted, it was previously determined that approximately 5% of Cu atoms were active in the conversion of methane to methanol over Cu/ZSM-5.⁹⁷ However, X-ray adsorption near edge structure

(XANES) studies have demonstrated that over Cu/MOR approximately 60% of Cu^{II} species change structure upon methane introduction and are reduced to Cu^{I} .^{130, 131} In a later contribution, it has been shown that the fraction of copper species that undergo reduction correlates well to the amount of methanol produced.¹³² It was also observed that multiple oxidation/reduction cycles were required to obtain a representative view of long-term performance of methane partial oxidation over Cu/MOR, as it is suggested that the copper species present equilibrate over many cycles.

Recent *operando* X-ray absorption spectroscopy (XAS) and high-energy-resolution fluorescence-detected (HERFD) XANES spectroscopy investigations into the active sites of Cu-exchanged MOR strongly suggest that the active species in the systems tested is a dicopper species.¹³³ This hypothesis is supported by two crucial pieces of evidence; first, a Cu-MOR material was tested in which approximately one methane molecule was activated for every two Cu ions within the material. Subsequently, the methanol productivity across a range of materials and reaction procedures was observed to increase with a slope of 0.5 as the concentration of what is identified spectroscopically as the active Cu species increases. Within this contribution, the highest methanol yield to date over Cu-modified zeolites is reported at $170\ \mu\text{mol}_{\text{MeOH}}\ \text{g}_{\text{cat}}^{-1}$ using a Cu-exchanged mordenite with $\text{Si}/\text{Al} = 7$ and $\text{Cu}/\text{Al} = 0.18$.¹³³

The presence of various counter cations has been shown to have a large effect on both the speciation of active sites within Cu/MOR and subsequent methanol productivity.^{121, 134, 135} It is broadly observed that Cu/MOR samples prepared by ion-exchange from a H-form parent zeolite perform better in terms of methanol productivity than those prepared from an alkali/alkaline earth metal exchanged parents (X-form, where $X = \text{Na}^+, \text{K}^+, \text{Mg}^{2+}, \text{Ca}^{2+}$), a phenomenon that is explained in two ways. Firstly, whilst H^+ ions exhibit a preference for exchange position within the 12MR channel of MOR, it is suggested that both Cu^{2+} and Na^+ ions exhibit a thermodynamic preference for exchange sites within the 8MR pore mouth and hence compete with one another for this exchange position.¹³⁴ It can therefore be assumed that the statistical likelihood of two or three Cu^{2+} ions existing within the 8MR at a proximity close enough to form multinuclear active site clusters is greatly diminished in X-form parents when compared to H-form parents.¹³⁴ This is supported by an observable decrease in methane conversion over Cu/MOR possessing various counter cations ($\text{Na}^+, \text{K}^+, \text{Mg}^{2+}, \text{Ca}^{2+}$) when compared to H^+ at similar copper concentrations. Secondly, it is argued that the presence of proximal Brønsted acid sites (H^+) increases stability of the produced methanol, preventing over-oxidation to carbon monoxide and dioxide.¹³⁵ This conclusion is drawn from an observed maximum methanol selectivity over Cu/MOR species containing the highest proportion of Brønsted acid sites.

2.2.4.3 Small-pore zeolites

Recently, copper-modified small pore zeolites, such as SSZ-13, have gained substantial interest as potential materials to facilitate methane partial oxidation.^{94, 113, 136} In particular,

Cu/SSZ-13 has been reported to produce competitive quantities of methanol per copper atom to both previously spotlighted zeolites, Cu/ZSM-5 and Cu/MOR, at similar Si:Al ratios.^{94, 109, 136} Much of the recent literature suggests that isolated copper ions, in the form of $[\text{CuOH}]^+$, are responsible for the transformation of methane to methanol over Cu/SSZ-13 (as mentioned in section 2.2.1) as opposed to the multinuclear clusters observed for larger-pore zeolites.^{105, 106, 133}

Importantly, Cu/SSZ-13 has not only been shown to produce methanol in the standard stepwise process, but has also shown great potential in a continuous regime utilising both O_2 ¹⁰⁹ and N_2O ¹³⁶ as oxidants. Maximum methane conversion and methanol production rates over Cu/SSZ-13 (H-form parent) and using N_2O as an oxidant were observed when employing a gas composition of 30% CH_4 , 30% N_2O , 3% H_2O (balance He) at 573 K, resulting in production of $55 \mu\text{mol}_{\text{MeOH}} \text{g}_{\text{cat}}^{-1} \text{h}^{-1}$. The greatest methanol selectivity, however, was observed at a lower temperature of 543 K and lower Cu loading, implying that at a higher temperature, selectivity is sacrificed for production rates.¹³⁶ When using O_2 as an oxidant and a feed gas mixture of $\text{CH}_4/\text{O}_2/\text{H}_2\text{O}$, the maximum yield recorded over several different frameworks was $3.12 \mu\text{mol}_{\text{MeOH}} \text{g}_{\text{cat}}^{-1} \text{h}^{-1}$ as a result of catalysis over Cu/CHA.¹⁰⁹

Given the potential realised for confinement to promote the partial oxidation of methane, we expect that additional progress in the field will be made by exploiting zeolites which have small pores or more importantly small channels and side pockets. For an in-depth review of 8MR zeolites, readers are suggested to see the excellent review by Dusselier and Davis.¹³⁷ Interestingly, until recently, the highest reported methanol yield to date, $86.1 \mu\text{mol}_{\text{MeOH}} \text{g}_{\text{cat}}^{-1}$, utilised zeolite omega (MAZ structure), which contains an intersecting 8MR small pore network alongside a discrete 12MR channel.⁹² However, this has now been surpassed once again by MOR which notably contains an 8MR side pocket.¹³³

2.3 Zn-modified zeolites

In 2004, Kazansky *et al.* reported heterolytic CH_4 bond dissociation over Zn exchanged zeolites.¹³⁸ Since then, a number of groups have gone on to show that methane can be partially oxidised in the presence of dioxygen over zinc modified zeolites. A major advantage of these zinc based systems is the ability to form an active species without an initial high temperature oxidation step, which is required for iron and copper modified zeolites. Hence, these materials are of great interest industrially as an isothermal process could be developed.

Framework bound Zn^{2+} cations are believed to be responsible for C-H activation but the mechanism involved is still highly debated. The zinc species introduced in to the zeolite is dependent on a number of factors: the zeolite topology, Si/Al ratio, method of zinc introduction and also any further thermal treatment carried out.¹³⁹

Two key ways of introducing zinc into zeolites are incipient wetness impregnation and ion exchange using a decomposable

zinc salt. These methods can introduce a variety of zinc species into the zeolite: isolated Zn^{2+} ions which sit at cation exchange sites within the zeolite, $[\text{Zn-O-Zn}]^{2+}$ clusters formed through the condensation of partially hydrolysed $[\text{Zn-OH}]^+$ extraframework ions and ZnO clusters, though ion exchange methods result in predominantly the introduction of Zn^{2+} cations.^{139, 140} The presence of multiple zinc species makes it difficult to determine which exact species is responsible for C-H activation and subsequently a variety of different mechanisms have been proposed.

Chemical vapour deposition (CVD) methods can also be used to introduce zinc into zeolites. Vapour deposition with Zn^0 powder involves the exchange of Brønsted acid sites (BAS) for Zn^{2+} ions *via* a redox reaction evolving H_2 .¹⁴¹ Under certain zinc vapour deposition conditions, additional zinc species have been detected. A small fraction of paramagnetic isolated Zn^+ ions have also been detected by EPR spectroscopy upon contact of metallic zinc vapours with H-ZSM-5.¹⁴² In the presence of large quantities of zinc, diamagnetic $[\text{Zn}_2]^{2+}$ dimers have also been observed which upon UV irradiation increases the number of Zn^+ ions present by one order of magnitude.¹⁴³ However, neither the Zn^+ species or $[\text{Zn}_2]^{2+}$ dimers have been reported to react with methane. CVD of dimethyl zinc leads to surface grafted $[\text{Zn-CH}_3]^+$ species which can be converted to Zn^{2+} ions through reaction with H_2 or oxidised to ZnO clusters.¹³⁹

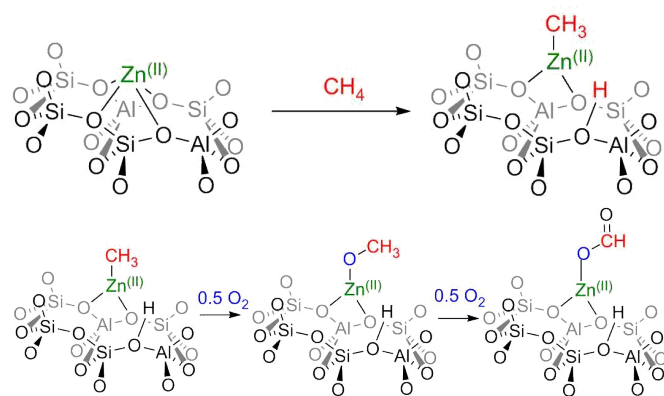
The levels of exchange can vary with the method of zinc introduction. Through collection of molecular H_2 produced upon zinc vapour deposition, Kasansky *et al.* showed that full exchange of BAS occurs.¹³⁸ Substitution through impregnation or ion exchange methods normally results in lower exchange levels.¹³⁹ This is particularly evident in high silica zeolites where there is a low framework charge and potentially a high degree of separation between Al tetrahedra. Reduced zinc loading is often ascribed to the difficulty of stabilising the formal 2+ charge associated with the Zn^{2+} ions in high silica zeolites.^{144, 140}

2.3.1 Mechanism of C-H activation in zinc exchanged zeolites

Understanding the mechanism of CH_4 activation in zinc exchanged zeolites is essential for the progress of the fundamental and applied chemistry of these materials. Zinc exchanged into the MFI micropore network, Zn/ZSM-5, has been the most studied system for C-H activation. However, the mechanism of activation is still under debate.

In 2004, Kazansky *et al.* were the first to report that heterolytic CH_4 bond dissociation can occur at room temperature on isolated Zn^{2+} sites in Zn/ZSM-5 as determined through diffuse reflectance infrared fourier transform spectroscopy (DRIFTS) studies, having observed the formation of a zinc methyl species and a framework BAS as demonstrated in Scheme 1.¹³⁸

Solid-state NMR spectroscopy has also been a key technique in confirming the formation of the Zn- CH_3 species. Kolyagin *et al.* were the first to observe a signal at $\delta = -20$ ppm from the reaction of CH_4 within Zn/ZSM-5 at ambient temperature.¹⁴⁵ The upfield chemical shift is characteristic of methyl groups in different organozinc compounds implying the



Scheme 1: Top: C–H activation step for dissociative adsorption of methane over Zn²⁺ forming a Zn–CH₃ and new BAS. Bottom: Formation of methoxy and formate species on Zn–CH₃ through addition of O₂.

presence of a surface zinc methyl.¹⁴⁶ The peak position was found to be independent of methane loading suggesting the presence of a well-defined surface species. The intensity of the line increased considerably in a ¹H–¹³C CP/MAS NMR spectrum in comparison to a direct excitation spectrum. This indicates the peak corresponds to a rigid surface species strongly attached to the surface. This evidence presented by Kolyagin *et al.* strongly suggests that methane activation at ambient temperature takes place by dissociative adsorption over Zn sites resulting in the formation of a Zn–CH₃ species and a framework BAS. DRIFTS and NMR spectroscopy have shown that upon initial exposure to methane, an intermediate is formed in which a methane molecule is adsorbed onto an isolated zinc cation.^{138, 147} Following thermal treatment, a C–H bond of this intermediate is heterolytically cleaved between the zinc centre and a framework oxygen atom. The Zn²⁺ species acts as a Lewis acid with the CH₄ σ(C–H) orbital donating electron density into the Zn–4s orbital, while the framework oxygen atom acts as a Lewis base, leading to C–H bond cleavage.¹¹⁷ This Zn²⁺ species at the mononuclear active sites, as opposed to other zinc species formed through ion exchange mechanisms, is also active for H₂ dissociation as shown through IR spectroscopy studies.¹¹⁷

However, other mechanistic theories have been presented using different active sites. A ¹³C NMR signal at δ = 58 ppm corresponding to a zinc methoxy species (ZnOCH₃) led Xu *et al.* to suggest homolytic C–H bond cleavage is possible over a [Zn–O–Zn]²⁺ cluster.¹⁴⁸ This Zn/ZSM-5 sample was interestingly prepared through Zn vapour deposition which should lead to the presence of predominantly Zn²⁺ ions only. The suggested mechanism involved the formation of a methyl radical (·CH₃) which can then interact with the zinc cluster to produce the zinc methoxy species. This zinc methoxy species was reportedly formed in a 3:1 ratio to the zinc methyl. As both species are present, Xu *et al.* suggests that both heterolytic cleavage over Zn²⁺ sites forming the zinc methyl species alongside the homolytic cleavage forming the methoxy species on [Zn–O–Zn]²⁺ dimer can occur, with the methoxy species being favoured according to the 3:1 ratio stated above.¹⁴⁸

The concept of both activation mechanisms, occurring simultaneously is supported by Wang *et al.* who also observed the presence of oxygenated species (methoxy and formate groups) whilst predominately observing the zinc methyl species in ZSM-5.¹⁴⁹ However, in this case, the zinc was introduced through incipient wetness impregnation which can lead to a variety of zinc species within the zeolite.¹⁴⁹ The signals from the methoxy and formate groups disappeared upon further heating of the sample implying additional reactions occurring at higher temperatures.

On the other hand, Stepanov *et al.* have provided strong evidence that the appearance of zinc methoxy and formate species are in fact not due to the radical based homolytic cleavage suggested above but actually due to the presence of adventitious oxygen shown in Scheme 1.¹⁴¹ When Zn/ZSM-5 prepared by vapour deposition was exposed to labelled methane (¹³CH₄) at room temperature, two signals at δ = –4 and –6 ppm, corresponding to physisorbed methane, were observed in the ¹³C NMR spectrum.¹⁴¹ The two signals correspond to two Zn²⁺ sites of different Lewis acidity caused by a non-homogeneous aluminium distribution.¹³⁸ Upon heating to 250 °C, the zinc methyl peak is observed as expected, in the absence of any methoxy or formate species. Oxygenated peaks only appeared through the addition of molecular oxygen at room temperature. The intensity of these NMR signals increased upon heating and the presence of NMR signals from further oxygenated species such as carbonates, ethers and aldehydes were also subsequently detected. This study therefore supports heterolytic cleavage as the principle method of CH₄ activation by Zn²⁺ ions contrary to the findings of Xu *et al.*

Understanding the role of Al distribution in zeolites is key to maximising metal-ion exchange levels. It has been determined that as few as 5–15% of ion-exchanged sites are active for CH₄ heterolysis in MFI zeolites.¹⁵⁰ Further, it has been reported that the same zinc active sites are able to activate both CH₄ and H₂.^{117, 150} DFT studies have suggested this reactivity is dependent on a specific Al array within the zeolite.¹⁵¹ A recent theoretical paper by Kuroda examines the spontaneous heterolytic cleavage of H₂ on Zn²⁺/MFI to investigate this dependence.¹⁵² It was found that heterolysis was more favourable on a circumferentially-arrayed Al–Al site compared with a straight channel axis in MFI as shown in Figure 10. This is due to the formation of a favourably aligned Lewis base–Zn²⁺ pair resulting in a suitable position to activate H₂, even at room temperature. Therefore, the Al arrangement alongside the curvature created by the zeolite pores may be seen to have an impact on the activity of metal ions within zeolite frameworks.

2.3.2 Zinc oxide clusters in Zeolites

Zinc oxide clusters in zeolites have been shown to be catalytically active for propane aromatisation.^{153, 154} Through *in situ* NMR spectroscopy studies, it has been observed that ZnO aggregates, alongside residual BAS, are active for propane aromatisation in a zinc impregnated BEA sample. This is proposed to occur *via* dissociative adsorption of propane on the ZnO species within the pores of the zeolite *via* cleavage of

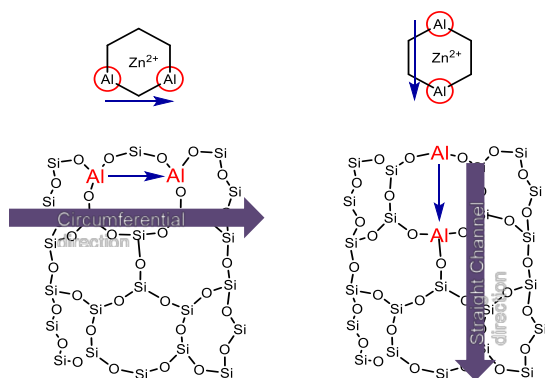


Figure 10: Representation of Al array direction within a zeolite framework: circumferential and straight channel directions. Adapted with permission from reference 150. Copyright 2017 Royal Society of Chemistry

a C–H bond.¹⁵³ ZnO clusters have been shown to promote ethane activation but are unable to catalyse the aromatisation of ethane which takes place primarily over Lewis acidic Zn^{2+} or $[\text{Zn}-\text{O}-\text{Zn}]^{2+}$ sites.¹⁵⁵ However, systemic studies of zinc oxide and Zn^{2+} in beta show that zinc oxide is unable to activate methane to form zinc methyl species.

Zinc sites are able to affect H/D exchange of CH_4/CD_4 in Zn/H–BEA with differing reactivity depending on the nature of the active site. Isolated Zn^{2+} cations show pronounced H/D exchange but ZnO clusters are also found to be active, with rate constants of $65 \times 10^{-5} \text{ g mol}^{-1} \text{ min}^{-1}$ and $1.2 \times 10^{-5} \text{ g mol}^{-1} \text{ min}^{-1}$ respectively.¹⁴⁰ This reactivity, however, is limited to H/D exchange with no reaction observed for the alkylation of benzene with methane over these ZnO clusters. On the other hand, Zn^{2+} cations in BEA were able to activate methane to form the zinc methyl species which showed further reactivity with benzene to form substituted aromatics.¹⁴⁷ Similarly, Kazansky *et al.* have found that ZnO clusters in Zn/Na–Y are unable to perform heterolytic dissociative adsorption of methane.¹⁵⁶ The clusters in Zn/Na–Y can be reduced to form isolated Zn^{2+} but this new site is also inactive for C–H cleavage of methane further indicating that the framework plays an important role in mediating the reaction.¹⁵⁴

2.3.3 The role of Brønsted acid sites in C–H activation

Stepanov *et al.* have reported that residual BAS after zinc exchange play an interesting role in C–H activation. If BAS are present after zinc exchange on H–ZSM–5, CH_4 activation has been shown to be reversible under reduced pressure.¹⁴¹ On the other hand, in a fully zinc exchanged ZSM–5 the Zn– CH_3 fragments remain intact after exposure to vacuum.¹⁵⁷

Conversely, Wu *et al.* found that no reformation of methane with evacuation on a bifunctional Zn/H–ZSM–5 zeolite prepared by impregnation methods.¹⁵⁸ This demonstrates that different methods of zinc introduction can have different reactivity or distribution of zinc species. Wu's sample prepared by impregnation had a variety of zinc species present whereas Stepanov's sample, which showed reversible

reactivity, is proposed to have mainly Zn^{2+} present, from zinc vapour deposition. DOI: 10.1039/C9DT00922A

The synergic effect between BAS and zinc Lewis acid sites impacts the temperature required for C–H activation. It has been observed that fully zinc exchanged zeolites require temperatures of 250 °C for activation to take place whereas partially exchanged systems are able to form zinc methyl species at room temperature indicating mechanistic differences caused by the presence of BAS.¹⁴¹

High field solid state NMR spectroscopy studies have shown that a synergic effect between BAS and zinc species can promote H/D exchange. In this study, the spatial proximity of these sites is crucial, requiring a BAS–Zn distance $< 3.5 \text{ \AA}$.¹⁵⁹ The enhanced activity of these zinc sites is due to an increase in Brønsted acidity through the spatial proximity between the Zn^{2+} ions and the Brønsted acidic protons of the zeolite. The local electron density on the Zn^{2+} cation is increased (decreasing the electron density on the oxygen atoms around the BAS) leading to a weakening of the interaction between bridging oxygen atoms and acidic protons, overall increasing the acidity of the Zn-modified zeolites.

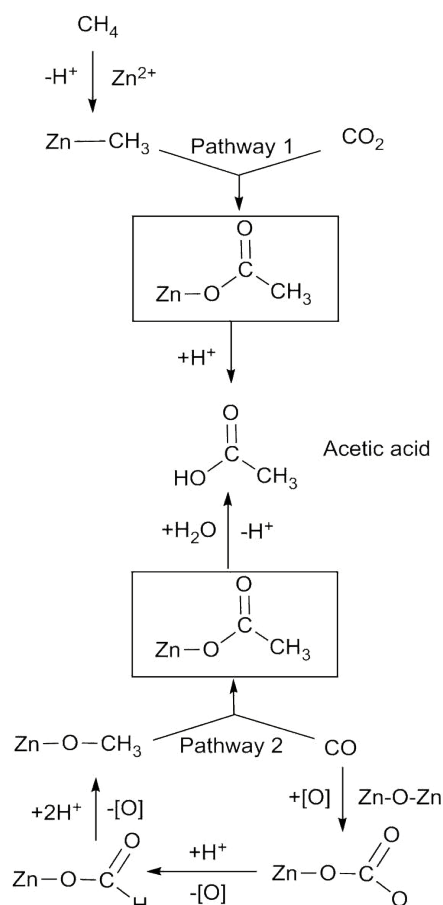
2.3.4 Reactivity of methane with small molecules on zinc-modified zeolites

As mentioned in Section 2.3.1, the formation of methoxy and formate groups are observed when the zinc methyl species are exposed to dioxygen. Reactivity has been observed at ambient temperature, whilst additional heating of the sample results in the formation of higher oxygenates such as acetic acid.^{141, 149} Further reactivity of zinc methyl species with molecules such as CO, CO_2 and H_2O has been explored by a number of groups and the chemical reactivity has been found to be very similar to that of organozinc compounds.^{141, 149, 158, 160}

In situ NMR spectroscopy studies by Deng *et al.* investigated the reactivity of the zinc methyl groups on Zn/H–ZSM–5.¹⁴⁹ Proton donors such as water, methanol and hydrochloride readily convert the zinc methyl species to methane at room temperature. Deng *et al.* found addition of oxygen to the methyl species results in formation of methoxy and formate groups at 300 °C, in agreement with the findings of Stepanov.^{141, 149} However, small substoichiometric amounts of methanol are also observed in the NMR spectrum.

The addition of CO and CO_2 to methane over zinc exchanged zeolites has been studied in the context of the formation of acetic acid (Scheme 2). Acetic acid can be formed through two different pathways: CO reacting with surface methoxy species or CO_2 reacting with zinc methyls.¹⁶¹ The BAS play a key role in the formation of acetic acid *via* proton transfer to the surface acetate species formed upon addition of CO_2 .¹⁵⁸

2.3.5 Differing reactivity between zinc and magnesium



Scheme 2: Proposed reaction pathways for the formation of acetic acid from methane and carbon monoxide on Zn/ZSM-5. Adapted with permission from reference 161. Copyright 2012 Wiley

Both Zn^{2+} and Mg^{2+} have similar ionic radii and charge, hence, similar reactivity towards the C–H bond of methane could be expected. However it has been shown that magnesium exchanged ZSM-5 does not form $[\text{Mg-CH}_3]^+$ species under identical conditions to those used for zinc exchanged ZSM-5.¹⁶² Furthermore, H_2 is also not readily chemisorbed on Mg/ZSM-5.¹⁵⁰ Kuroda *et al.* investigated these reactivity differences through IR spectroscopy studies involving the adsorption of CH_4 and CO on Mg/ZSM-5 and Zn/ZSM-5 samples supported by DFT calculations.¹⁶² Stronger perturbation of the adsorbed CH_4 molecule at room temperature was observed through interaction with Zn^{2+} compared with Mg^{2+} . Upon heating, the presence of a zinc methyl group was detected but no change in the IR spectrum of Mg/ZSM-5 was observed. As the electrostatic force of Zn^{2+} is almost identical to that of Mg^{2+} , the authors suggest that the higher activation of the C–H bond observed for Zn^{2+} is due to an electron-transfer interaction rather than based on electrostatics. Similarly, when CO was used as a probe molecule and adsorption studies were undertaken. These studies determined that for Mg^{2+} (and group 2 ions in general), CO adsorption is predominantly governed by electrostatic interaction. However, zinc behaves as an electron acceptor for the CO molecule (as well as for the CH_4 molecule) and this electron-accepting nature is the key electronic feature for CH_4

heterolytic activation. DFT calculations supported that CH_4 dissociation over monomeric Zn^{2+} is derived from the greater electron-accepting power than Mg^{2+} cations.

2.4 Other d-block metals in zeolites

2.4.1 Cobalt-modified zeolites

Unlike the previous metals discussed (Fe, Cu, Zn), the literature surrounding the partial oxidation of methane to methanol over Co-modified zeolites is relatively sparse. There are two major products of methane partial oxidation over Co-modified zeolites, methanol and formaldehyde, and their relative selectivities depend upon the active Co species. Cobalt oxide species, Co_3O_4 and CoO, throughout the zeolite are typically selective towards methanol production whilst Co^{2+} cations within the zeolite channels show a general selectivity towards formaldehyde production.¹⁶³ As a result, the effect of modification method on methanol selectivity over Co/ZSM-5 may be dramatic; it was found that Co/ZSM-5 prepared by incipient wetness impregnation (IWI) typically contains more surface Co oxide species and is more selective towards methanol, whilst Co/ZSM-5 prepared *via* ion exchange (IE) contains more Co^{2+} species within the zeolite channel system and is more selective towards formaldehyde.¹⁶³

It has been reported that increasing the surface area of Co/ZSM-5 by the introduction of mesoporosity *via* alkaline treatment can improve methanol selectivity by increasing the number of potential Co oxide sites.^{164, 165} A contribution from Beznis *et al.* shows that a linear correlation between the zeolite surface area and number of Co oxide species can be established and (owing to the selectivity for methanol of Co oxides) a linear correlation between zeolite surface area and methanol selectivity also results.¹⁶⁴ The authors also suggested that increased methanol selectivity could be attributed to the reduced ability to form Co^{2+} sites as a result of extra-framework alumina blocking the channel system. Hence, a subsequent acid treatment to remove extra-framework alumina was applied to the previously alkali treated zeolites before Co introduction. As expected, the relative amounts of Co^{2+} species within the zeolite channels increased and methanol selectivity decreased.¹⁶⁴

Partial oxidation of methane conducted in a small-scale batch reactor at 150 °C under an atmosphere of methane (0.75 bar) and 5% oxygen in nitrogen (2 bar) respectively demonstrated the effect of exposure time and oxygen presence on the direct conversion of methane to methanol over Co-impregnated mesoporous H-ZSM-5.¹⁶⁶ It was found that the optimum extracted methanol yield (79%) was obtained at a reaction time of 60 minutes with longer reaction times resulting in a substantial decrease in yield which the authors suggest may be resultant from complete oxidation of methane to CO_2 and water. It is further suggested that the presence of molecular oxygen as an oxidant causes an increased reaction rate when compared to the base reaction in which oxygen (O^{2-}) from cobalt oxides or the ZSM-5 surface acts as the oxidising agent.

In all reports, a preliminary calcination step is required to introduce active oxygen species into Co modified zeolite materials (similar to Cu, *vide supra*) before being exposed to methane at 150 °C. Additionally, it is worth noting that the reaction products remain strongly adsorbed to the catalyst and must be extracted into the liquid phase resulting in a process that, at present, has not been demonstrated to run in a continuous regime.

DFT studies of the direct oxidation of methane to methanol over Co/ZSM-5 in the presence of N₂O have determined a reaction mechanism similar to that observed for α-Fe species.¹⁶⁷ Co/ZSM-5 is predicted to efficiently decompose N₂O resulting in an α-O species which is highly reactive towards radical hydrogen abstraction from methane. The mechanism follows the same pathway as that for Fe (*vide supra*) but with notably lower activation barriers for each step. As with Fe, the presence of water substantially decreases the energy barrier to the methanol formation step.

2.4.2 Other d-block modified zeolites.

In addition to the species covered in detail above, several other d-block metal modified zeolite catalysts have been reported to form analogous active sites to those discussed above or activate methane and hence have potential as methane-to-methanol catalysts, although many reports are discrete.

Ni-modified ZSM-5 has been reported to be active for the direct production of methanol from methane with an anchored mono(μ-oxo)nickel, [Ni₂(μO)]²⁺, motif reported as the active site, analogous to that observed for Cu-ZSM-5.¹⁶⁸ The zeolite must be thermally activated in O₂ before methane introduction but produces methanol as the major product at 150 °C, after aqueous extraction into the liquid phase from the catalyst. DFT studies, however, suggest that this active site motif is not plausible, as no activity in methane to methanol conversion was able to be simulated under reasonable conditions.¹⁶⁹ This conclusion corroborates with a recent contribution that utilises DFT+U calculations to simulate an array of plausible Ni-oxo motifs in the periodic MFI framework structure, namely [NiO]²⁺, [Ni₂(μO)]²⁺, [Ni₂(μO)₂]²⁺, and [Ni₃(μO)₃]²⁺ (Figure 11).¹⁷⁰ It is suggested that the reactivity of the [Ni₂(μO)]²⁺ centre is insufficient to be the active site owing to its respective energy of activation for hydrogen atom abstraction from methane being both considerably higher than that observed experimentally and that calculated for the other motifs examined.^{168, 170} Conversely, the energy of activation for hydrogen atom abstraction calculated for the [Ni₂(μO)₂]²⁺, and

[Ni₃(μO)₃]²⁺ centres is in good agreement with that observed experimentally. Furthermore, the authors suggest that, based on the calculated values for energy of methanol desorption for both active sites, the energetics are within the range that may enable spontaneous, solvent-free and online product extraction.¹⁷⁰ As alluded to in the contribution, the use of experimental resonance Raman spectroscopy (rR) (as used to discern the active species in Cu-modified zeolites) could prove invaluable in assigning the true nature of the active Ni species.

Finally, Mn/ZSM-5 has been shown to be active in the decomposition of N₂O resulting in the suggested formation of an α-O species.¹⁷¹ Similar to Fe/ZSM-5, this site cannot be generated directly using O₂. At the time of writing, no activation of methane (or any other alkane) over this species has been reported, however the suggested similarity to the α-O in Fe/ZSM-5 could prove promising in methane partial oxidation.

3. Outlook and Areas for Future Research

The development of zeolite based, dMtM catalysts that can compete with the existing two step syngas pathway, remains a major challenge though significant progress has been made in the last 20 years. Competing with the established syngas technology, which has been honed for decades through a combination of chemistry and chemical engineering, will require further substantial effort from the industrial and academic communities. It should be stressed that dMtM technology may not have to compete with the syngas route under certain scenarios; in the monetisation of associated natural gas or other waste methane sources, where it is simply too impractical and/or costly to build a syngas plant and a methanol plant.

At the present time, the single, major improvement that is required to help push dMtM forward as a technology is in preventing unwanted over oxidation to carbon oxides. This remains a major challenge as avoiding thermodynamic fate is no mean feat. However, zeolites are known to give reaction products that differ from thermodynamic predictions (e.g. toluene alkylation with methanol to p-xylene over ZSM-5)¹⁷² and it stands that zeolites may be able to confer the desired reaction selectivities in dMtM. Conceptually, we believe this could be achieved with metal exchanged zeolite catalysts by exploiting the strategies below which either complement or build on some of the strategies recently suggested by others.^{31, 38-40}

Confinement Zeolites are well known to be able to impart reaction selectivities that differ from those predicted by thermodynamics alone. In the case of dMtM it is unlikely that *product selectivity* will contribute to improving the selectivity of the reaction due to the similar size of the reactant and the product. On the other hand, exploiting *confinement effects* which can lower the transition state barrier to C-H activation would enable better activation kinetics and lower process operation temperature. To this end, confinement has very recently been experimentally shown to accelerate methane

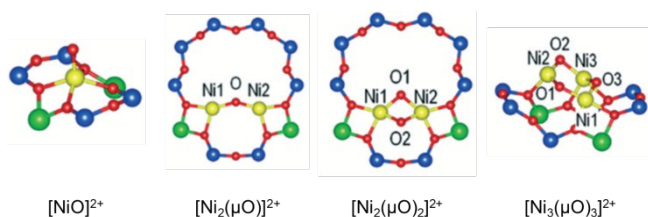


Figure 11: Optimised ground state structures of [NiO]²⁺, [Ni₂(μO)]²⁺, [Ni₂(μO)₂]²⁺, and [Ni₃(μO)₃]²⁺ in MFI. Adapted with permission from reference 170. Copyright 2018 Royal Society of Chemistry

activation over copper oxide clusters in the MOR framework²³ whilst theoretical studies support this approach for further study.⁷⁷ Additionally, it is necessary for *confinement effects* not to accelerate the activation of the methanol product which could be mitigated by further strategies outlined below.

1e⁻ vs 2e⁻ Processes The mechanism of methane oxidation to methanol by the vast majority of materials mentioned in this perspective operate *via* a radical based C–H bond activation process. These 1e⁻ processes are now well understood to result in low methanol selectivities due to the weaker C–H bond of methanol being kinetically more reactive and resulting in over oxidation.^{33, 38} In the case of functionalisation by 2e⁻ processes, this need not be true. For example, where a sigma complex is formed prior to C–H bond cleavage (e.g. activation by Lewis acid and base or electrophilic activation by transition metals), the more electron rich C–H bond of methane favours coordination, and thus subsequent activation, over the relatively electron poor C–H bond of methanol. Therefore developing and exploring systems where methane complex formation precedes bond cleavage (such as methane activation by Lewis acid-base pairs over zinc exchanged ZSM-5)^{147,173} should be a target for future endeavours. In the homogeneous Shilov system, which is capable of converting methane to methanol under remarkably mild conditions (120 °C, in water), the C–O bond forming reaction occurs by nucleophilic attack (a 2e⁻ process) of water at the carbon atom of a Pt(IV)–CH₃ group.³⁰ While thermodynamics exclude water as a viable oxidant, it highlights alternative mechanisms for C–O bond formation and shows that activation and functionalisation could potentially be separated from a cycle involving dioxygen. This would be akin to the Wacker process, the industrially practised method of acetaldehyde production from ethylene and dioxygen. The process is catalysed by Pd and Cu chloride salts in an acidic, aqueous solution and the C–O bond is in fact formed from water, not dioxygen.¹⁷⁴

Hydrophobic pockets This strategy has been advocated by Román-Leshkov³⁹ as well as Nørskov,³⁸ and has parallels in the *modus operandi* of MMO enzymes. In order to prevent over oxidation, rapid release and diffusion of methanol away from the active site is paramount. The non-polar nature of methane compared to the polar and hydrogen bonding properties of methanol can in principle be exploited to engender reaction selectivity. This suggests that ionic active sites (i.e. metal-exchanged, aluminosilicate zeolites) may be unsuitable. However, it is conceivable that neutral frameworks with Lewis acid framework sites could serve to activate alkanes. Additionally, minimising diffusion paths indicates that the rapidly developing fields of nano-zeolites¹⁷⁵ and hierarchical zeolites¹⁷⁶ may have a role to play in improving the conversion / selectivity paradigm. In connection, due to the high solubility of methanol in water, recent theoretical work proposes that enhanced reaction selectivity should be observed for dMtM when conducted in water compared to the gas phase, and this is supported by experimental studies.³⁸

Theoretical studies As has been outlined in this perspective, theoretical studies are making substantial

contributions to the field, providing insight into kinetic mechanistic and thermodynamic considerations (see for example recent contributions from Nørskov,^{38, 177} Yoshizawa¹⁷⁸ and Sievers⁴⁰). As exemplified and explicitly mentioned by Nørskov,³⁸ most of these studies are connected to the prevalent radical based, 1e⁻ processes. Additionally, accurate modelling of long-range electrostatic interactions and dispersion in zeolite catalysis is now recognised as key to determining accurate theoretical activation energies. [Bell Catalysis Today 2018 312, P51] Therefore we believe there is substantial scope for theoretical studies to explore 2e⁻ based methane activation and functionalisation processes over metal-exchanged zeolites, and also to explore how the framework can confer optimised confinement effects, both areas for further experimental research that have been highlighted in this section above.

In summary, there remains much to be achieved in dMtM research, though we believe it is likely that zeolites incorporating 3d transition metals will play a prominent role in bringing this long standing challenge to fruition.

Conflicts of interest

There are no conflicts to declare.

Acknowledgements

M.S. and S.R. thank the EPSRC and Durham University for generous financial support for their PhD studentships. R.T. thanks the EPSRC for generous funding of an EPSRC Manufacturing Fellowship (grant number EP/R01213X/1).

References

1. BP Energy Outlook, <https://www.bp.com/en/global/corporate/media/press-releases/energy-outlook-2018.html>, (accessed 9th November, 2018).
2. K. Aasberg-Petersen, I. Dybkjær, C. V. Ovesen, N. C. Schjødt, J. Sehested and S. G. Thomsen, *J. Nat. Gas Sci. Eng.*, 2011, **3**, 423-459.
3. K. Aasberg-Petersen, J. H. Bak Hansen, T. S. Christensen, I. Dybkjær, P. S. Christensen, C. Stub Nielsen, S. E. L. Winter Madsen and J. R. Rostrup-Nielsen, *Appl. Catal., A*, 2001, **221**, 379-387.
4. S. C. Reyes, J. H. Sinfelt and J. S. Feeley, *Ind. Eng. Chem. Res.*, 2003, **42**, 1588-1597.
5. R. Reimert, F. Marschner, H.-J. Renner, W. Boll, E. Supp, M. Brejc, W. Liebner and G. Schaub, in *Gas Production 2. Processes, Ullmann's Encyclopedia of Industrial Chemistry*, Wiley-VCH Verlag GmbH & Co. KGaA, 2011.
6. S. A. Bhat and J. Sadhukhan, *AIChE J.*, 2009, **55**, 408-422.
7. J. Ott, V. Gronemann, F. Pontzen, E. Fiedler, G. Grossmann, D. B. Kersebohm, G. Weiss and C. Witte, in *Methanol, Ullmann's Encyclopedia of Industrial Chemistry*, Wiley-VCH Verlag GmbH & Co. KGaA, 2012.
8. W. A. Bone and R. V. Wheeler, *J. Chem. Soc., Trans.*, 1902, **81**, 535-549.

ARTICLE

Journal Name

9. C. Elvidge, M. Zhizhin, K. Baugh, F.-C. Hsu and T. Ghosh, *Energies*, 2016, **9**, 14.
10. BGR, *Energy Study 2013. Reserves, resources and availability of energy resources*, Hannover, 2013.
11. G. L. Foster, D. L. Royer and D. J. Lunt, *Nat. Commun.*, 2017, **8**, 14845.
12. P. G. Levi and J. M. Cullen, *Environ. Sci. Technol.*, 2018, **52**, 1725-1734.
13. OECD Environmental Outlook to 2030, (accessed 12th November, 2018).
14. *World Energy Outlook 2017*, IEA publications, 2017.
15. E. V. Kondratenko, T. Peppel, D. Seeburg, V. A. Kondratenko, N. Kalevaru, A. Martin and S. Wohlrab, *Catal. Sci. Technol.*, 2017, **7**, 366-381.
16. Siluria Technologies, http://siluria.com/Technology/Demonstration_Plant, (accessed 15th November 2018).
17. Siluria Technologies, http://siluria.com/Newsroom/Press_Releases, (accessed 15th November 2018).
18. B. A. Arndtsen, R. G. Bergman, T. A. Mobley and T. H. Peterson, *Acc. Chem. Res.*, 1995, **28**, 154-162.
19. V. C. C. Wang, S. Maji, P. P. Y. Chen, H. K. Lee, S. S. F. Yu and S. I. Chan, *Chem. Rev.*, 2017, 8574-8621.
20. M. O. Ross and A. C. Rosenzweig, *J. Biol. Inorg. Chem.*, 2017, **22**, 307-319.
21. Z. Zakaria and S. K. Kamarudin, *Renew. Sust. Energ. Rev.*, 2016, **65**, 250-261.
22. P. Tomkins, M. Ranocchiari and J. A. van Bokhoven, *Acc. Chem. Res.*, 2017, **50**, 418-425.
23. B. E. R. Snyder, M. L. Bols, R. A. Schoonheydt, B. F. Sels and E. I. Solomon, *Chem. Rev.*, 2018, **118**, 2718-2768.
24. R. Manoj, R. Marco and v. B. J. A., *Angew. Chem., Int. Ed.*, 2017, **56**, 16464-16483.
25. N. J. Gunsalus, A. Koppaka, S. H. Park, S. M. Bischof, B. G. Hashiguchi and R. A. Periana, *Chem. Rev.*, 2017, **117**, 8521-8573.
26. A. I. Olivos-Suarez, À. Szécsényi, E. J. M. Hensen, J. Ruiz-Martinez, E. A. Pidko and J. Gascon, *ACS Catal.*, 2016, **6**, 2965-2981.
27. W. Taifan and J. Baltrusaitis, *Appl. Catal., B Environ.*, 2016, **198**, 525-547.
28. C. Karakaya and R. J. Kee, *Progr. Energy Combust. Sci.*, 2016, **55**, 60-97.
29. J. A. Labinger, *Chem. Rev.*, 2017, **117**, 8483-8496.
30. J. A. Labinger and J. E. Bercaw, *J. Organomet. Chem.*, 2015, **793**, 47-53.
31. M. Ravi, M. Ranocchiari and J. A. van Bokhoven, *Angew. Chem., Int. Ed.*, 2017, **56**, 16464-16483.
32. J. A. Labinger and J. E. Bercaw, *Nature*, 2002, **417**, 507-514.
33. J. A. Labinger, *J. Mol. Catal. A: Chem.*, 2004, **220**, 27-35.
34. M. Lersch and M. Tilset, *Chem. Rev.*, 2005, **105**, 2471-2526.
35. C. L. Rasmussen and P. Glarborg, *Ind. Eng. Chem. Res.*, 2008, **47**, 6579-6588.
36. H. D. Gesser, N. R. Hunter and C. B. Prakash, *Chem. Rev.*, 1985, **85**, 235-244.
37. A. E. Shilov and G. B. Shul'pin, *Chem. Rev.*, 1997, **97**, 2879-2932.
38. A. A. Latimer, A. Kakekhani, A. R. Kulkarni and J. K. Nørskov, *ACS Catal.*, 2018, **8**, 6894-6907.
39. K. T. Dinh, M. M. Sullivan, P. Serna, R. J. Meyer, M. Dincă and Y. Román-Leshkov, *ACS Catal.*, 2018, **8**, 8306-8313.
40. J. N. Jocz, A. J. Medford and C. Sievers, *ChemCatChem*, 2019, **11**, 593-600.
41. W. A. Bone and R. V. Wheeler, *J. Chem. Soc., Trans.*, 1903, **83**, 1074-1087.
42. FR352687, 1905.
43. T. E. Layng and R. Soukup, *Ind. Eng. Chem.*, 1928, **20**, 1052-1055.
44. N. F. Gol'dshleger, M. B. Tyabin, A. E. Shilov and A. A. Shteinman, *Zh. Fiz. Khim.*, 1969, **18**, 2174-2175.
45. N. F. Gol'dshleger, V. V. Es'kova, A. E. Shilov and A. A. Shteinman, *Zh. Fiz. Khim.*, 1972, **46**, 1353-1354.
46. R. A. Periana, D. J. Taube, S. Gamble, H. Taube, T. Satoh and H. Fujii, *Science*, 1998, **280**, 560-564.
47. M. M. Konnick, S. M. Bischof, M. Yousufuddin, B. G. Hashiguchi, D. H. Ess and R. A. Periana, *J. Am. Chem. Soc.*, 2014, **136**, 10085-10094.
48. T. Zimmermann, M. Soorholtz, M. Bilke and F. Schüth, *J. Am. Chem. Soc.*, 2016, **138**, 12395-12400.
49. T. Zimmermann, M. Bilke, M. Soorholtz and F. Schüth, *ACS Catal.*, 2018, **8**, 9262-9268.
50. L. F. Albright, *Ind. Eng. Chem. Res.*, 2009, **48**, 1409-1413.
51. J. T. Grant, J. M. Venegas, W. P. McDermott and I. Hermans, *Chem. Rev.*, 2018, **118**, 2769-2815.
52. M. H. Mahyuddin, A. Staykov, Y. Shiota and K. Yoshizawa, *ACS Catal.*, 2016, **6**, 8321-8331.
53. N. D. Spencer and C. J. Pereira, *J. Catal.*, 1989, **116**, 399-406.
54. K. J. Zhen, M. M. Khan, C. H. Mak, K. B. Lewis and G. A. Somorjai, *J. Catal.*, 1985, **94**, 501-507.
55. S. Y. Chen and D. Willcox, *Ind. Eng. Chem. Res.*, 1993, **32**, 584-587.
56. N. D. Spencer, *J. Catal.*, 1988, **109**, 187-197.
57. O. Kiyoshi and H. Masaharu, *Chem. Lett.*, 1992, **21**, 2397-2400.
58. T. Weng and E. E. Wolf, *App. Cat. A: Gen.*, 1993, **96**, 383-396.
59. C. A. G. Fajardo, D. Niznansky, Y. N'Guyen, C. Courson and A.-C. Roger, *Catal. Commun.*, 2008, **9**, 864-869.
60. US4918249A, 1990.
61. S. Han, E. A. Kaufman, D. J. Martenak, R. E. Palermo, J. A. Pearson and D. E. Walsh, *Catal. Lett.*, 1994, **29**, 27-32.
62. US3529020A, 1970.
63. V. I. Sobolev, K. A. Dubkov, O. V. Panna and G. I. Panov, *Catal. Today*, 1995, **24**, 251-252.
64. A. Klerk, *Energ. Sci. Eng.*, 2015, **3**, 60-70.
65. W. Vermeiren and J.-P. Gilson, *Top. Catal.*, 2009, **52**, 1131-1161.
66. R. Millini and G. Bellussi, in *Zeolites in Catalysis: Properties and Applications*, The Royal Society of Chemistry, 2017, pp. 1-36.
67. R. Gounder and E. Iglesia, *Chem. Commun.*, 2013, **49**, 3491-3509.
68. A. Corma, *J. Catal.*, 2003, **216**, 298-312.
69. A. Bhan, A. D. Allian, G. J. Sunley, D. J. Law and E. Iglesia, *J. Am. Chem. Soc.*, 2007, **129**, 4919-4924.
70. B. Li, J. Xu, B. Han, X. Wang, G. Qi, Z. Zhang, C. Wang and F. Deng, *J. Phys. Chem. C*, 2013, **117**, 5840-5847.
71. G. I. Panov, V. I. Sobolev and A. S. Kharitonov, *J. Mol. Catal.*, 1990, **61**, 85-97.

Journal Name

ARTICLE

72. G. I. Panov, G. A. Sheveleva, A. S. Kharitonov, V. N. Romannikov and L. A. Vostrikova, *Appl. Catal., A*, 1992, **82**, 31-36.
73. V. I. Sobolev, A. S. Kharitonov, Y. A. Paukshtis and G. I. Panov, *J. Mol. Catal.*, 1993, **84**, 117-124.
74. G. I. Panov, V. I. Sobolev, K. A. Dubkov, V. N. Parmon, N. S. Ovanesyan, A. E. Shilov and A. A. Shteinman, *React. Kinet. Catal. Lett.*, 1997, **61**, 251-258.
75. E. V. Starokon, M. V. Parfenov, L. V. Pirutko, S. I. Abornev and G. I. Panov, *J. Phys. Chem. C*, 2011, **115**, 2155-2161.
76. B. E. R. Snyder, P. Vanelderren, M. L. Bols, S. D. Hallaert, L. H. Böttger, L. Ungur, K. Pierloot, R. A. Schoonheydt, B. F. Sels and E. I. Solomon, *Nature*, 2016, **536**, 317.
77. F. Göttl, C. Michel, P. C. Andrikopoulos, A. M. Love, J. Hafner, I. Hermans and P. Sautet, *ACS Catal.*, 2016, **6**, 8404-8409.
78. E. V. Starokon, M. V. Parfenov, S. S. Arzumanov, L. V. Pirutko, A. G. Stepanov and G. I. Panov, *J. Catal.*, 2013, **300**, 47-54.
79. Y. K. Chow, N. F. Dummer, J. H. Carter, R. J. Meyer, R. D. Armstrong, C. Williams, G. Shaw, S. Yacob, M. M. Bhasin, D. J. Willock, S. H. Taylor and G. J. Hutchings, *ChemPhysChem*, 2018, **19**, 402-411.
80. J. Valyon, W. S. Millman and W. K. Hall, *Catal. Lett.*, 1994, **24**, 215-225.
81. J. Leglise, J. O. Petunchi and W. K. Hall, *J. Catal.*, 1984, **86**, 392-399.
82. P. C. Andrikopoulos, Z. Sobalik, J. Novakova, P. Sazama and S. Sklenak, *ChemPhysChem*, 2013, **14**, 520-531.
83. C. M. Fu, V. N. Korchak and W. K. Hall, *J. Catal.*, 1981, **68**, 166-171.
84. M. L. Bols, S. D. Hallaert, B. E. R. Snyder, J. Devos, D. Plessers, H. M. Rhoda, M. Dusselier, R. A. Schoonheydt, K. Pierloot, E. I. Solomon and B. F. Sels, *J. Am. Chem. Soc.*, 2018, **140**, 12021-12032.
85. B. Michalkiewicz, *Appl. Catal., A*, 2004, **277**, 147-153.
86. C. Hammond, M. M. Forde, M. H. Ab Rahim, A. Thetford, Q. He, R. L. Jenkins, N. Dimitratos, J. A. Lopez-Sanchez, N. F. Dummer, D. M. Murphy, A. F. Carley, S. H. Taylor, D. J. Willock, E. E. Stangland, J. Kang, H. Hagen, C. J. Kiely and G. J. Hutchings, *Angew. Chem. Int. Edit.*, 2012, **51**, 5129-5133.
87. C. Hammond, R. L. Jenkins, N. Dimitratos, J. A. Lopez-Sanchez, M. H. ab Rahim, M. M. Forde, A. Thetford, D. M. Murphy, H. Hagen, E. E. Stangland, J. M. Moulijn, S. H. Taylor, D. J. Willock and G. J. Hutchings, *Chem. – Eur. J.*, 2012, **18**, 15735-15745.
88. C. Hammond, N. Dimitratos, R. L. Jenkins, J. A. Lopez-Sanchez, S. A. Kondrat, M. Hasbi ab Rahim, M. M. Forde, A. Thetford, S. H. Taylor, H. Hagen, E. E. Stangland, J. H. Kang, J. M. Moulijn, D. J. Willock and G. J. Hutchings, *ACS Catal.*, 2013, **3**, 689-699.
89. C. Hammond, N. Dimitratos, J. A. Lopez-Sanchez, R. L. Jenkins, G. Whiting, S. A. Kondrat, M. H. ab Rahim, M. M. Forde, A. Thetford, H. Hagen, E. E. Stangland, J. M. Moulijn, S. H. Taylor, D. J. Willock and G. J. Hutchings, *ACS Catal.*, 2013, **3**, 1835-1844.
90. J. Xu, R. D. Armstrong, G. Shaw, N. F. Dummer, S. J. Freakley, S. H. Taylor and G. J. Hutchings, *Catal Today*, 2016, **270**, 93-100.
91. M. H. Groothaert, P. J. Smeets, B. F. Sels, P. A. Jacobs and R. A. Schoonheydt, *J. Am. Chem. Soc.*, 2005, **127**, 1394-1395.
92. M. B. Park, S. H. Ahn, A. Mansouri, M. Ranocchiari and J. A. van Bokhoven, *ChemCatChem*, 2017, **9**, 3705-3713.
93. P. J. Smeets, M. H. Groothaert and R. A. Schoonheydt, *Catal Today*, 2005, **110**, 303-309.
94. M. J. Wulfers, S. Teketel, B. Ipek and R. F. Lobo, *Chem Commun*, 2015, **51**, 4447-4450.
95. M. H. Groothaert, J. A. van Bokhoven, A. A. Battiston, B. M. Weckhuysen and R. A. Schoonheydt, *J. Am. Chem. Soc.*, 2003, **125**, 7629-7640.
96. M. H. Groothaert, K. Lievens, J. A. van Bokhoven, A. A. Battiston, B. M. Weckhuysen, K. Pierloot and R. A. Schoonheydt, *ChemPhysChem*, 2003, **4**, 626-630.
97. J. S. Woertink, P. J. Smeets, M. H. Groothaert, M. A. Vance, B. F. Sels, R. A. Schoonheydt and E. I. Solomon, *Proc. Nat. Acad. Sci.*, 2009, **106**, 18908-18913.
98. R. S. Czernuszewicz, J. E. Sheats and T. G. Spiro, *Inorg. Chem.*, 1987, **26**, 2063-2067.
99. M. H. Groothaert, K. Lievens, H. Leeman, B. M. Weckhuysen and R. A. Schoonheydt, *J. Catal.*, 2003, **220**, 500-512.
100. P. J. Smeets, R. G. Hadt, J. S. Woertink, P. Vanelderren, R. A. Schoonheydt, B. F. Sels and E. I. Solomon, *J. Am. Chem. Soc.*, 2010, **132**, 14736-14738.
101. M. L. Tsai, R. G. Hadt, P. Vanelderren, B. F. Sels, R. A. Schoonheydt and E. I. Solomon, *J. Am. Chem. Soc.*, 2014, **136**, 3522-3529.
102. S. Grundner, M. A. C. Markovits, G. Li, M. Tromp, E. A. Pidko, E. J. M. Hensen, A. Jentys, M. Sanchez-Sanchez and J. A. Lercher, *Nat. Commun.*, 2015, **6**, 7546.
103. G. Li, P. Vassilev, M. Sanchez-Sanchez, J. A. Lercher, E. J. M. Hensen and E. A. Pidko, *J. Catal.*, 2016, **338**, 305-312.
104. D. Palagin, A. J. Knorpp, A. B. Pinar, M. Ranocchiari and J. A. van Bokhoven, *Nanoscale*, 2017, **9**, 1144-1153.
105. C. Paolucci, A. A. Parekh, I. Khurana, J. R. Di Iorio, H. Li, J. D. Albarracin Caballero, A. J. Shih, T. Anggara, W. N. Delgass, J. T. Miller, F. H. Ribeiro, R. Gounder and W. F. Schneider, *J. Am. Chem. Soc.*, 2016, **138**, 6028-6048.
106. A. R. Kulkarni, Z.-J. Zhao, S. Siahrostami, J. K. Nørskov and F. Studt, *ACS Catal.*, 2016, **6**, 6531-6536.
107. F. Giordanino, P. N. R. Vennestrøm, L. F. Lundegaard, F. N. Stappen, S. Mossin, P. Beato, S. Bordiga and C. Lamberti, *Dalton Trans.*, 2013, **42**, 12741-12761.
108. E. Borfecchia, K. A. Lomachenko, F. Giordanino, H. Falsig, P. Beato, A. V. Soldatov, S. Bordiga and C. Lamberti, *Chem. Sci.*, 2015, **6**, 548-563.
109. K. Narsimhan, K. Iyoki, K. Dinh and Y. Román-Leshkov, *ACS Cent. Sci.*, 2016, **2**, 424-429.
110. P. Vanelderren, J. Vancauwenbergh, B. F. Sels and R. A. Schoonheydt, *Coordin. Chem. Rev.*, 2013, **257**, 483-494.
111. Z.-J. Zhao, A. Kulkarni, L. Vilella, J. K. Nørskov and F. Studt, *ACS Catal.*, 2016, **6**, 3760-3766.
112. E. M. C. Alayon, M. Nachtegaal, A. Bodi and J. A. van Bokhoven, *ACS Catal.*, 2014, **4**, 16-22.
113. R. Oord, J. E. Schmidt and B. M. Weckhuysen, *Catal. Sci. Technol.*, 2018, **8**, 1028-1038.
114. M. H. Mahyuddin, T. Tanaka, Y. Shiota, A. Staykov and K. Yoshizawa, *ACS Catal.*, 2018, **8**, 1500-1509.

ARTICLE

Journal Name

115. P. Tomkins, A. Mansouri, S. E. Bozbag, F. Krumeich, B. Park Min, E. M. C. Alayon, M. Ranocchiari and J. A. van Bokhoven, *Angew. Chem., Int. Ed.*, 2016, **55**, 5467-5471.
116. T. Sheppard, C. D. Hamill, A. Goguet, D. W. Rooney and J. M. Thompson, *Chem. Commun.*, 2014, **50**, 11053-11055.
117. A. Oda, H. Torigoe, A. Itadani, T. Ohkubo, T. Yumura, H. Kobayashi and Y. Kuroda, *J. Phys. Chem. C*, 2013, **117**, 19525-19534.
118. V. L. Sushkevich, D. Palagin, M. Ranocchiari and J. A. van Bokhoven, *Science*, 2017, **356**, 523-527.
119. R. A. Periana, *Science*, 2017, **358**.
120. J. A. Labinger, *Science*, 2018, **359**.
121. V. L. Sushkevich, D. Palagin and J. A. v. Bokhoven, *Angew. Chem., Int. Ed.*, 2018, **57**, 8906-8910.
122. M. A. C. Markovits, A. Jentys, M. Tromp, M. Sanchez-Sanchez and J. A. Lercher, *Top. Catal.*, 2016, **59**, 1554-1563.
123. N. V. Beznis, B. M. Weckhuysen and J. H. Bitter, *Catal. Lett.*, 2010, **138**, 14-22.
124. P. Vanelderen, B. E. R. Snyder, M.-L. Tsai, R. G. Hadt, J. Vancauwenbergh, O. Coussens, R. A. Schoonheydt, B. F. Sels and E. I. Solomon, *J. Am. Chem. Soc.*, 2015, **137**, 6383-6392.
125. B. E. R. Snyder, P. Vanelderen, R. A. Schoonheydt, B. F. Sels and E. I. Solomon, *J. Am. Chem. Soc.*, 2018, **140**, 9236-9243.
126. E. G. Derouane, *J. Catal.*, 1986, **100**, 541-544.
127. P. Cheung, A. Bhan, G. J. Sunley and E. Iglesia, *Angew. Chem., Int. Ed.*, 2006, **45**, 1617-1620.
128. A. J. Jones, S. I. Zones and E. Iglesia, *J. Phys. Chem. C*, 2014, **118**, 17787-17800.
129. M. L. Sarazen, E. Duskocil and E. Iglesia, *ACS Catal.*, 2016, **6**, 7059-7070.
130. E. M. C. Alayon, M. Nachtegaal, M. Ranocchiari and J. A. van Bokhoven, *CHIMIA Int. J. Chem.*, 2012, **66**, 668-674.
131. M. A. Newton, A. J. Knorpp, A. B. Pinar, V. L. Sushkevich, D. Palagin and J. A. van Bokhoven, *J. Am. Chem. Soc.*, 2018, 10090-10093.
132. S. E. Bozbag, E. M. C. Alayon, J. Pecháček, M. Nachtegaal, M. Ranocchiari and J. A. van Bokhoven, *Catal. Sci. Technol.*, 2016, **6**, 5011-5022.
133. D. K. Pappas, A. Martini, M. Dyballa, K. Kvande, S. Teketel, K. A. Lomachenko, R. Baran, P. Glatzel, B. Arstad, G. Berlier, C. Lamberti, S. Bordiga, U. Olsbye, S. Svelle, P. Beato and E. Borfecchia, *J. Am. Chem. Soc.*, 2018, 15270-15278.
134. S. Grundner, W. Luo, M. Sanchez-Sanchez and J. A. Lercher, *Chem. Commun.*, 2016, **52**, 2553-2556.
135. V. L. Sushkevich and J. A. v. Bokhoven, *Catal. Sci. Technol.*, 2018, **8**, 4141-4150.
136. B. Ipek and R. F. Lobo, *Chem. Commun.*, 2016, **52**, 13401-13404.
137. M. Dusselier and M. E. Davis, *Chem. Rev.*, 2018, 5265-5329.
138. V. B. Kazansky and A. I. Serykh, *Phys. Chem. Chem. Phys.*, 2004, **6**, 3760-3764.
139. S. M. T. Almutairi, B. Mezari, P. C. M. M. Magusin, E. A. Pidko and E. J. M. Hensen, *ACS Catal.*, 2012, **2**, 71-83.
140. I. Pinilla-Herrero, E. Borfecchia, J. Holzinger, U. V. Mentzel, F. Joensen, K. A. Lomachenko, S. Bordiga, C. Lamberti, G. Berlier, U. Olsbye, S. Svelle, J. Skibsted and P. Beato, *J. Catal.*, 2018, **362**, 146-163.
141. A. A. Gabrienko, S. S. Arzumanov, M. V. Luzgin, A. G. Stepanov and V. N. Parmon, *J. Phys. Chem. C*, 2015, **119**, 24910-24918.
142. E. Morra, G. Berlier, E. Borfecchia, S. Bordiga, P. Beato and M. Chiesa, *J. Phys. Chem. C*, 2017, **121**, 14238-14245.
143. A. Oda, T. Ohkubo, T. Yumura, H. Kobayashi and Y. Kuroda, *Dalton Trans.*, 2015, **44**, 10038-10047.
144. A. Dyer and T. I. Emms, *J. Mater. Chem.*, 2005, **15**, 5012-5021.
145. Y. G. Kolyagin, I. I. Ivanova, V. V. Ordonsky, A. Gedeon and Y. A. Pirogov, *J. Phys. Chem. C*, 2008, **112**, 20065-20069.
146. H. Elmar, *Z. Anorg. Allg. Chem.*, 2000, **626**, 2223-2227.
147. M. V. Luzgin, D. Freude, J. Haase and A. G. Stepanov, *J. Phys. Chem. C*, 2015, **119**, 14255-14261.
148. J. Xu, A. Zheng, X. Wang, G. Qi, J. Su, J. Du, Z. Gan, J. Wu, W. Wang and F. Deng, *Chem. Sci.*, 2012, **3**, 2932-2940.
149. J. F. Wu, W. D. Wang, J. Xu, F. Deng and W. Wang, *Chem. - Eur. J.*, 2010, **16**, 14016-14025.
150. A. Oda, H. Torigoe, A. Itadani, T. Ohkubo, T. Yumura, H. Kobayashi and Y. Kuroda, *Angew. Chem., Int. Edit.*, 2012, **51**, 7719-7723.
151. E. A. Pidko and R. A. van Santen, *J. Phys. Chem. C*, 2007, **111**, 2643-2655.
152. A. Oda, T. Ohkubo, T. Yumura, H. Kobayashi and Y. Kuroda, *Phys. Chem. Chem. Phys.*, 2017, **19**, 25105-25114.
153. A. A. Gabrienko, S. S. Arzumanov, D. Freude and A. G. Stepanov, *J. Phys. Chem. C*, 2010, **114**, 12681-12688.
154. A. A. Gabrienko, S. S. Arzumanov, A. V. Toktarev, I. G. Danilova, I. P. Prosvirin, V. V. Kriventsov, V. I. Zaikovskii, D. Freude and A. G. Stepanov, *ACS Catal.*, 2017, **7**, 1818-1830.
155. A. Mehdad and R. F. Lobo, *Catal. Sci. Technol.*, 2017, **7**, 3562-3572.
156. V. B. Kazansky, V. Yu. Borovkov, A. I. Serykh, R. A. van Santen and P. J. Stobbelaar, *Phys. Chem. Chem. Phys.*, 1999, **1**, 2881-2886.
157. A. G. Stepanov, S. S. Arzumanov, A. A. Gabrienko, V. N. Parmon, I. I. Ivanova and D. Freude, *ChemPhysChem*, 2008, **9**, 2559-2563.
158. J.-F. Wu, S.-M. Yu, W. D. Wang, Y.-X. Fan, S. Bai, C.-W. Zhang, Q. Gao, J. Huang and W. Wang, *J. Am. Chem. Soc.*, 2013, **135**, 13567-13573.
159. G. Qi, Q. Wang, J. Xu, J. Trébosc, O. Lafon, C. Wang, J.-P. Amoureux and F. Deng, *Angew. Chem., Int. Ed.*, 2016, **55**, 15826-15830.
160. Y. Lin, S. Qi, L. Benedict, Z. Junlin, K. Dejing, M. Claire, T. Chiu and T. Edman, *Angew. Chem., Int. Ed.*, 2017, **56**, 10711-10716.
161. X. Wang, G. Qi, J. Xu, B. Li, C. Wang and F. Deng, *Angew. Chem., Int. Ed.*, 2012, **51**, 3850-3853.
162. A. Oda, H. Torigoe, A. Itadani, T. Ohkubo, T. Yumura, H. Kobayashi and Y. Kuroda, *J. Phys. Chem. C*, 2014, **118**, 15234-15241.
163. N. V. Beznis, B. M. Weckhuysen and J. H. Bitter, *Catal. Lett.*, 2010, **136**, 52-56.
164. N. V. Beznis, A. N. C. van Laak, B. M. Weckhuysen and J. H. Bitter, *Micropor. Mesopor. Mat.*, 2011, **138**, 176-183.
165. Y. K. Krisnandi, B. A. P. Putra, M. Bahtiar, Zahara, I. Abdullah and R. F. Howe, *Procedia Chem.*, 2015, **14**, 508-515.

Journal Name

ARTICLE

166. Y. K. Krisnandi, B. A. Samodro, R. Sihombing and R. F. Howe, *Indones. J. Chem.*, 2015, **15**, 263-268.
167. M. F. Fellah and I. Onal, *J. Phys. Chem. C*, 2010, **114**, 3042-3051.
168. J. Shan, W. Huang, L. Nguyen, Y. Yu, S. Zhang, Y. Li, A. I. Frenkel and F. Tao, *Langmuir*, 2014, **30**, 8558-8569.
169. A. A. Arvidsson, V. P. Zhdanov, P.-A. Carlsson, H. Gronbeck and A. Hellman, *Catal. Sci. Technol.*, 2017, **7**, 1470-1477.
170. M. H. Mahyuddin and K. Yoshizawa, *Catal. Sci. Technol.*, 2018, 5875-5885.
171. D. Radu, P. Glatzel, A. Gloter, O. Stephan, B. M. Weckhuysen and F. M. F. de Groot, *J. Phys. Chem. C*, 2008, **112**, 12409-12416.
172. J. P. Breen, R. Burch, M. Kulkarni, D. McLaughlin, P. J. Collier and S. E. Golunski, *Appl. Catal., A*, 2007, **316**, 53-60.
173. S. S. Arzumanov, A. A. Gabrienko, D. Freude and A. G. Stepanov, *Catal. Sci. Technol.*, 2016, **6**, 6381-6388.
174. J. A. Keith and P. M. Henry, *Angew. Chem., Int. Ed.*, 2009, **48**, 9038-9049.
175. S. Mintova, J.-P. Gilson and V. Valtchev, *Nanoscale*, 2013, **5**, 6693-6703.
176. K. Möller and T. Bein, *Chem. Soc. Rev.*, 2013, **42**, 3689-3707.
177. A. A. Latimer, A. R. Kulkarni, H. Aljama, J. H. Montoya, J. S. Yoo, C. Tsai, F. Abild-Pedersen, F. Studt and J. K. Nørskov, *Nat. Mater.*, 2017, **16**, 225-229.
178. M. H. Mahyuddin, Y. Shiota, A. Staykov and K. Yoshizawa, *Acc. Chem. Res.*, 2018, **51**, 2382-2390.

View Article Online
DOI: 10.1039/C9DT00922A

